Vorticity Formulations for Predicting the Flow of Incompressible Fluid

Mr Adam James Brierley

Submitted for the Degree of M.Sc.

Centre for Computational Engineering Sciences
Cranfield University,
Cranfield, Bedfordshire, MK43 0AL,
United Kingdom

2025

Except where acknowledged in the customary manner, the material presented in this thesis is, to the best of my knowledge, original and has not been submitted in whole or part for a degree in any university.

_____

Mr Adam James Brierley

CRANFIELD UNIVERSITY

Centre for Computational Engineering Sciences

M.Sc. Thesis

Academic Year: 2024-2025

Mr Adam James Brierley

Vorticity Formulations for Predicting the Flow of Incompressible Fluid

Supervisor:

Dr. László Könözsy

Abstract

Two solvers based on the *vorticity-formulations* for solving the flow of an incompressible fluid have been written. The first has used the streamfunction-vorticity (ψ-Ω) formulation and the latter the vector potential-vorticity ($\vec{\psi}$-$\vec{\Omega}$) formulation. The test case used to validate the solvers was the lid driven square and cubic cavity, respectively. Investigations into the physics of these problems was also carried out. The primary aim was to develop the $\vec{\psi}$-$\vec{\Omega}$ formulation. There are numerous advantages to the $\vec{\psi}$-$\vec{\Omega}$ approach over other well-known formulations, as well as certain difficulties. The main difficulty is enforcing the the divergence-free vorticity constraint.

A solid foundation has been laid for further development of the $\vec{\psi}$-$\vec{\Omega}$ formulation. This formulation has potential to be extended to complex geometries and to be highly optimised. Eventually, a direct numerical simulation (DNS) code using the $\vec{\psi}$-$\vec{\Omega}$ formulation may be developed, which may have the potential to discover new physics or find significant applications in industry. The author has found this subject to be intellectually stimulating and there is no end to the potential investigations in this topic.

Results showed good agreement with the literature for quantities like the centreline velocities for Reynolds' numbers 100, 400, and 1000 for the $\vec{\psi}$-$\vec{\Omega}$ solver. There is discrepancy, but this is only due to poorly optimised simulation parameters and time limitations. The primary issue remains divergence of vorticity, in future this may be tackled in a variety of different ways.

Acknowledgements

I would like to thank Dr. László Könözsy for his patience and oversight during this thesis and for introducing me to such an interesting topic. The freedom to bend the initial parameters and to develop my own personal solver was much appreciated. Furthermore, this thesis has seemlessly integrated with modules taught by Dr. Könözsy to the end that I have gained a deep knowledge of fluid mechanics, although I am aware I have only just scratched the surface. I hope to pursue this topic further in future and to become an expert in the field of incompressible fluid flows. My next goal is to go deeper into the mathematics.

I would also like to thank my parents for their support throughout my life which has enabled me to reach this point, and their continued support.

Adam Brierley

Contents

List of Figures

List of Tables

Nomenclature

Symbol	Unit	Description
a	m/s	Speed of sound (in a particular fluid medium)
$\vec{a}, \vec{b}$	-	Generic vectors
C	-	Arbitrary constant
$\vec{e}_x, \vec{e}_y, \vec{e}_z$	-	Unit vectors in the x, y, and z directions
$\vec{g}$	m/s^2	Vector field of gravity
i, j, k	-	Indices for nodes in the x, y, and z directions
Ma	-	Dimensionless Mach number (problem dependent)
n	-	Unit vector in the normal direction
nx, ny	-	Number of nodes in the x and y direction
R	$J/kg \cdot K$	Gas constant for a fluid medium
Re	-	Non-dimensional Reynolds' number
t	s	Time
T	K	Scalar field of temperature, $T = T(x, y, z; t)$
$\vec{u}$	m/s	Vector field of velocity, $\vec{u} = \vec{u}(x, y, z; t)$
u_c	m/s	Characteristic velocity
u_∞	m/s	Reference velocity
u, v, w	m/s	Scalar components of the velocity vector field
x, y, z	m	Cartesian coordinates
$\Delta\varepsilon$	-	Error
μ	$Pa \cdot s$	Dynamic viscosity
Π	J	Total potential of mechanical energy
ρ	kg/m^3	Scalar field of fluid density, $\rho = \rho(x, y, z; t)$
τ_1, τ_2	-	Tangential unit vectors
Φ	m^2/s	Scalar potential
ψ	m^2/s	Scalar field of the streamfunction, $\psi = \psi(x, y; t)$
$\vec{\Omega}$	s^{-1}	Vector field of vorticity, $\vec{\Omega} = \vec{\Omega}(x, y, z; t)$
Ω_x, Ω_y, Ω_z	s^{-1}	Scalar components of the vorticity vector field

Abbreviations

AC	Artificial Compressibility
DNS	Direct Numerical Simulation
FD	Finite Difference
FE	Finite Element
FS-PP	Fractional-Step Pressure-Projection
FV	Finite Volume
PDE	Partial Differential Equation
P-P	Pressure-Projection
SIMPLE	Semi-Implicit Method for Pressure-Linked Equations
$\psi - \Omega$	Streamfunction-Vorticity
$\vec{\psi} - \vec{\Omega}$	Vector Potential-Vorticity

Operators

Symbol	Description
∇	Hamilton (nabla), vector-type differential operator, $\nabla = \left(\frac{\partial}{\partial x}\vec{e}_x + \frac{\partial}{\partial y}\vec{e}_y + \frac{\partial}{\partial z}\vec{e}_z\right)$
∇^2	Laplacian, scalar-type differential operator, $\nabla^2 = \left(\frac{\partial^2}{\partial x^2} + \frac{\partial^2}{\partial y^2} + \frac{\partial^2}{\partial z^2}\right)$
$\otimes$	Dyad or tensor product of two second-rank tensors
$\cdot$	Scalar or inner or 'dot' product of two vectors

Chapter 1

Introduction and Objectives

1.1 Background and Motivation

The vector potential-vorticity formulation is an alternative and promising approach to the solution of flows of incompressible fluid. Whilst it has been attempted as a formulation in the past, there were computational limitations as well as difficulties with the formulation. In light of current computational power it is a good time to revisit the formulation as an alternative to popular approaches, such as the SIMPLE algorithm or the primitive variable approach.

One advantage is that the divergence-free constraint on the velocity field is automatically satisfied as part of the physical formulation. In effect, the vorticity is governing the dynamics of the flow whilst the vector potential is assuring adherence to the incompressibility constraint.

Another desirable feature of this approach is that there is a direct link between the governing equations and physical processes, such as the stretching of vorticity. This fact gives the formulation good future potential to investigate topics such as instability, transition, and turbulence, with opportunity to uncover new physics.

1.2 Problem Statement

The aim of this thesis is to write the foundation of a vector potential-vorticity code ready for further developments and advances. This was achieved, and the code has been validated against the known benchmark of the lid driven cubic cavity. Part of this process was understanding and learning the physics of these problems. Also, as the project developed

it became more and more mathematical in nature. It was an opportunity to begin to dive deeper into mathematics. It was also a chance to develop my own solvers, that is using the $\psi - \Omega$ and $\vec{\psi} - \vec{\Omega}$ formulations, which is the first time I have written full solvers myself. With this I had to tackle the associated challenges, especially with regards to accuracy and speed, and storing and processing results in an organised, efficient, and presentable manner. Overall it was a very valuable experience.

The project has laid the foundation for future developments in this area, with a future priority to have a full DNS solver implementing the vector potential-vorticity formulation.

1.3 Structure of the M.Sc. Thesis

- Chapter 1 - Introduction and Objectives - the background and the motivation for writing a vector potential-vorticity formulation solver.
- Chapter 2 - Literature Review - a literature review covering respectively the $\psi - \Omega$ formulation and the application of this method to a lid driven square cavity problem, and the $\vec{\psi} - \vec{\Omega}$ formulation with its application to the three dimensional cubic cavity problem.
- Chapter 3 - Governing Equations and Methods of Computation - the governing equations and methodology for incompressible fluid flows *in general*.
- Chapter 4 - The $\psi - \Omega$ formulation - the governing equations and methodology for the $\psi - \Omega$ formulation, including derivation of the vorticity transport equation, boundary conditions, the algorithm, and a link to the public repository housing the code.
- Chapter 5 - The Lid-Driven Cavity in Two Dimensions - the results of the $\psi - \Omega$ solver as applied to the two dimensional lid driven cavity problem.
- Chapter 6 - The Vector Potential-Vorticity Formulation - the governing equations and methodology for the $\vec{\psi} - \vec{\Omega}$ formulation, including the algorithm, boundary conditions, and a link to the public repository housing the code.
- Chapter 7 - The Three-Dimensional Lid-Driven Cube - the results of the $\vec{\psi} - \vec{\Omega}$ solver as applied to the lid driven cubic cavity problem.
- Chapter 8 - Future Work - discussions about future work and next steps.

Chapter 2

Literature Review

The development of the methods used in this thesis has been a collaborative effort spanning much of the past two centuries and beyond. This was just to get us to this point. Indeed, the streamfunction concept was introduced by Helmholtz and Lamb when they were studying classical hydrodynamics in the 19th century [3] [4]. By the early 20th century the streamfunction was a common analytical tool. The vorticity transport equation was also well known by the early 20th century, largely due to figures like Prandtl who popularised thinking in terms of vorticity [5]. In terms of the combined $\psi - \Omega$ formulation, this appeared with the emergence of computational fluid mechanics in the 1950s -1960s which was happening around the early computers in the US and around Los Alamos. To a great extent this early emergence of computational fluid mechanics was pioneered by John von Neumann who was working at this interface. By the 1960s the $\psi - \Omega$ formulation was a well established approach for incompressible fluid flows in two dimensions. Several other works were key in the development of the $\psi - \Omega$ formulation, for example Thom's 1933 paper [6].

2.1 The $\psi - \Omega$ Formulation

A popular test case used to validate the $\psi - \Omega$ formulation is the lid driven square cavity, and this is the approach taken in this thesis. To validate the solver, we must understand the physics of this problem. The first recorded numerical investigations into the two dimensional lid driven cavity were by Kawaguti in 1961 for the Physical Society of Japan [1] and by Burggraf in 1966 [2]. Kawaguti explored a Reynolds' number range of 0 (Stokes' or 'creeping' flow) through 128, and faced difficulties at Re = 128. In his case, the lid was moving from right to left as shown in figure 2.1.

It is enlightening to look at the earliest cases, both to see how things have developed

since that time, and to put our work into a historical perspective.

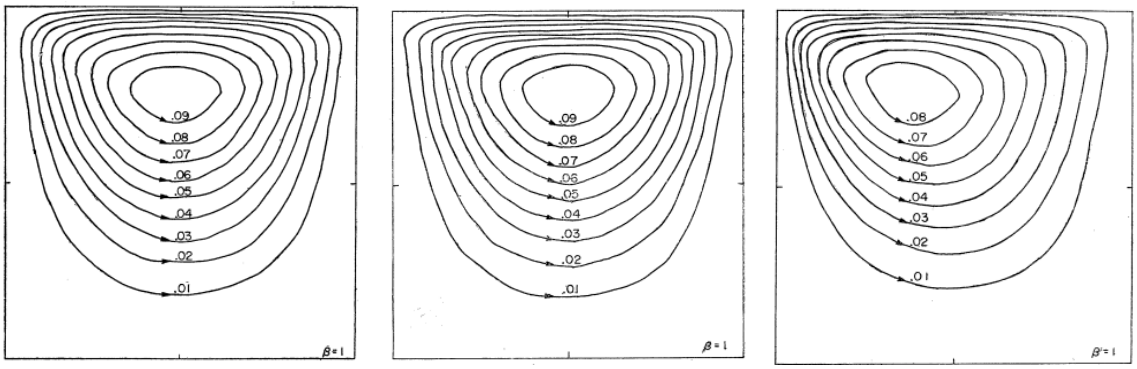

(a) Re = 0 (b) Re = 8 (c) Re = 64

Figure 2.1: The results of Kawaguti [1]

Kawaguti was studying the flow structure of viscous fluid as a function of Reynolds' number, with a mesh size of 11^2 nodes or 10 x 10 cells. He used a fourth order scheme on the interior points, and plotted streamlines, equi-vorticity lines, and isobaric lines, as well as centreline velocity and pressure distributions. Notedly, he was using the *steady* Navier-Stokes' equation. It is interesting to note that he reports a simulation time of approximately twenty minutes (running the same case on my personal computer today, with a finer grid of 21 x 21, takes less than ten seconds).

The streamlines in figure 2.1 show the contours along which the velocity vectors are parallel. Figure 2.1c shows the distortion of the vortex core toward the downstream corner due to the combined effects of continuity and viscosity, and the relative low influence of inertia. Kawaguti highlighted an issue when the Reynolds number was 128 and his solution did not converge. He hypothesised at that time that the divergence was likely due to a coarse grid, the inherent nature of the Navier-Stokes' equation, or the difference method implemented.

In terms of flow physics, he describes a circulating flow in the centre of the cavity, extending its whole length. He notes that relative to the pressure at the centre of the base of the cavity, the pressure on the downstream wall is high and the pressure on the upstream wall is low. Crucially, he does not report any secondary flow in the lower corners for Re < 64, but he maintains that this may be due to inaccuracy of the computation.

Though Kawaguti had been first to compute and report this problem by numerical solution, Burggraf's analysis is much more sophisticated [2]. This is especially because he combines the advantages of analytical approach with numerical solution. His concern is

with the viscous structure of the *recirculating* separated eddy in general, and separated flows more broadly. Indeed he notes that separated flows are an ancient field of study having been observed by great names such as da Vinci and Sir Isaac Newton. The lid driven cavity case provides a framework to study separated flow in isolation.

First, he calculates an analytical solution based on a linearised model and with a recirculating eddy bounded by a circular streamline. This reveals a completely viscous recirculating eddy at low *Re* which then develops an inviscid core at higher *Re*. This was envisaged by Batchelor [7]. This inviscid core becomes significant for a *Re* greater than 100. Whilst the vortex is still viscous, Burggraf finds that the vortex centre is distorted towards the upper downstream corner in accordance with Kawaguti. At higher *Re*, the now inviscid vortex core is more symmetrical about the centre of the circle as inertial terms have come to dominate most of the flow field (see figure 2.2c). Burggraf presents his results for Re = 0 - 400, and validity of the linear analysis is proven against the numerical solution which uses the $\psi - \Omega$ formulation.

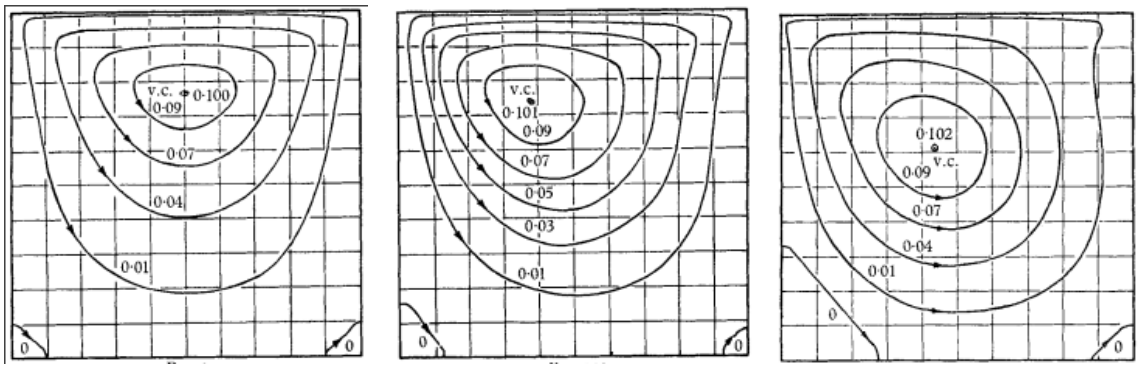

(a) Re = 0 (b) Re = 100 (c) Re = 400

Figure 2.2: The streamlines of Burggraf [2]

Despite the attention, separated flow remains an unsolved problem. Burggraf's investigation seeks to determine the structure of the recirculating eddy as a function of *Re*, just as many have tried when studying the separated flow in the wake of a cylinder. Crucially, he notes that transition points with *Re* are by no means set in stone, and that the results are strongly dependent upon the experimental conditions. He states that there are analytical approaches available for low *Re* to determine transition points, but even these are non-trivial. Numerical approaches, on the other hand, benefit from solving the entire equation.

Burggraf describes Batchelor's model of the separated recirculating eddy which is for a steady flow, and which assumes viscous effects are restricted to a thin layer along the

separation streamline [7]. This in turn causes a uniform vorticity core. Subsequent authors, such as Kuhlmann, have called it the 'Prandtl-Batchelor theorem' because it makes use of the thin viscous layer concept of Prandtl [5] [8]. It is also called the 'uniform vorticity model', because of the uniform vorticity centre. Some authors have questioned the assumption of a viscous separating layer due to the appearance of secondary vortices. Batchelor's model can be seen to describe the primary recirculating eddy, with secondary eddies also developing inviscid cores at higher *Re*. The corner eddies cascade down to smaller and smaller scales with increasing *Re* with the larger eddies gradually gaining an inviscid core [11].

As a result of the analytical analysis for a circular bounding streamline, Burggraf finds the velocity profiles across the separated eddy as displayed in figure 2.3. He claims that the structure within the main eddy is most clearly shown by a graph of the velocity profile across the eddy. He emphasises that viscous effects permeated the entire eddy for Kawaguti's flow regime, whilst his solutions pass into the inviscid regime. He observes a rounded profile for low *Re*, and a flattened profile for greater *Re*, where the flattened parts are representing the inviscid region. The slope of the flattened region, he reports, remains the same across *Re*, though its extent varies markedly.

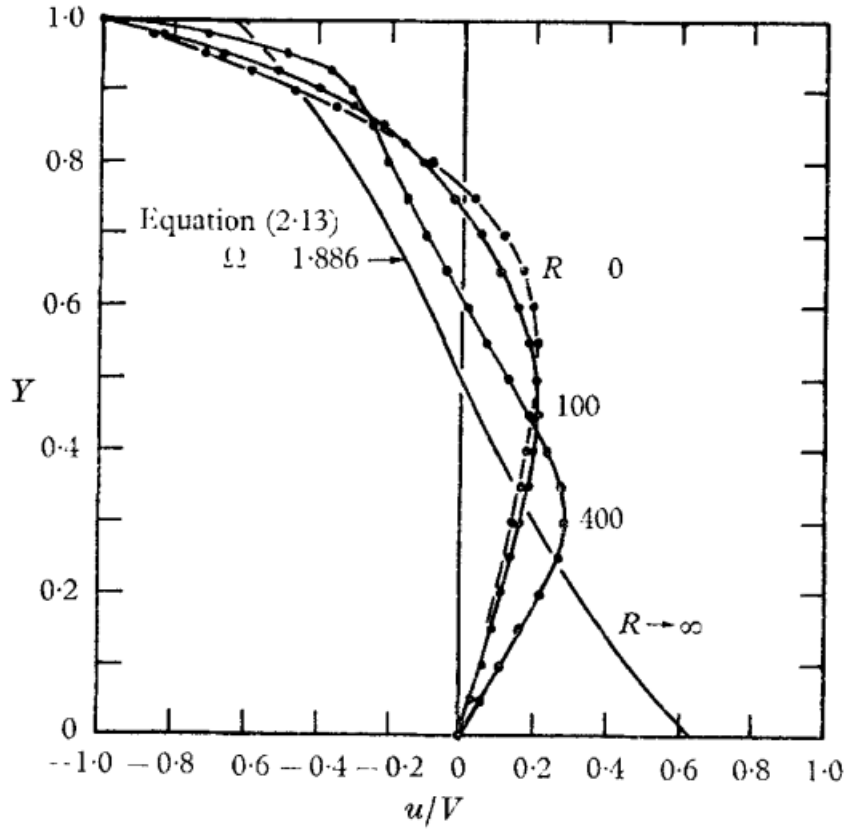

Figure 2.3: Burggraf centrelines [2].

Burggraf notes that there is strong variation in vorticity along the top and downstream walls of the cavity, indicating viscosity. He highlights that as *Re* increases, so must the mesh size decrease owing to diminishing thickness of the viscous layer near the wall. He also notes that near the wall "the interaction of convection and viscous diffusion of vorticity in the viscous annulus is indicated by the 'stretching' of the contours in the direction of flow". Burggraf concludes that total pressure distributions are the best indicator of the degree of viscous and inviscid flow, and again this is useful to note. Crucially, compared to Kawaguti he observes secondary flow in the corners for all *Re*, likely due to a finer grid, and notes that the pressure gradient may be particularly involved in these structures.

Furthermore, he emphasises that the solution near the singularities at the upper corners is locally identical to the scraping-corner solution treated by Taylor [10]. "Taylor explains this paradoxical situation arguing that the viscous stress will tend to lift the moving wall, creating a gap and so relieving the corner stresses". Burggraf notes this does not explain the case in which the moving wall recedes from the fluid.

Burggraf concludes that there is accord between his analytical and numerical approach. He comments that the vorticity contours give a better indication of the viscosity than streamlines, and had interesting points about residual viscosity in the inviscid vortex centre; maybe these plots are helpful in that regard.

He credits Moffat who studied the existing infinite series of contra-rotating eddies in the lower corners, that decrease in size and strength as the corner is approached [11]. These secondary eddies are originally completely viscous in nature. But, Burggraf states that the larger secondary eddies will become inviscid as *Re* increases, with inviscid eddies passing to smaller and smaller corner eddies.

2.2 The $\vec{\psi} - \vec{\Omega}$ Formulation

Weinan and Liu were the first to conduct the vector potential-vorticity method on a non-staggered grid [9]. Their focus is on tackling the issue of vorticity divergence. They take two approaches which differ in implementation of the normal component of the vorticity boundary condition, using a second and fourth order accurate scheme. Weinan and Liu observe the structure of the error and the effect of how the convective terms are discretised at the boundary. They also inspect the effect of the vorticity divergence on the overall accuracy, covering $Re = 500$ and 3200 for a cubic cavity flow and drawing comparisons with the MAC method. They find good agreement with the MAC method.

Weinan and Liu comment that most previous work was done on staggered grids. But this presents limitations when using nonrectangular grids. They derive a three dimensional analogue of local vorticity boundary conditions using Thom's formula. Clearly as a result of their work, discretisation of the convective term near the boundary and the scheme used for the vorticity boundary condition has the greatest impact on the vorticity divergence.

It is noted that the divergence of vorticity, velocity, and vector potential must be enforced. In this method, the divergence of velocity is automatically satisfied, as Weinan and Liu state that the divergence of vector potential is a consequence of divergence of vorticity. Thus the divergence of vorticity condition is paramount. They comment that most discretisation techniques result in Gibbs-like phenomena at the edges where the flow becomes singular, making the method intractable at high *Re*.

The subject of the paper is to prove an alternative form of writing the governing equa-

tions to facillitate different discretisation strategies particularly for the convective term. Some mathematical conclusions result from this. One, that though the streamfunction is uniquely defined the vector potential is not, and $\psi + \nabla\zeta$ will satisfy $\vec{u} = \nabla \times \psi$ as well as ψ, if ζ is a smooth scalar function. This is called the gauge freedom. The gauge freedom is fixed by maintaining the Poisson equation between $\vec{\Omega}$ and $\vec{\psi}$, which requires that $\nabla \cdot \vec{\psi} = 0$. Interestingly, Weinan and Liu state that if the divergence of $\vec{\psi}$ is zero on the boundary, then it may also be zero on the internal domain. This may also be true of other variables and is worth noting.

2.2.1 Cubic Cavity

In terms of the cubic cavity, Kuhlmann [8] notes that in two dimensions there are the difficulties of the top corner singuarities which is Taylor's scraping problem [10] and the lower corner which are Moffat eddies [11]. Kuhlmann states that a three dimensional corner with a moving wall, such as dealt with in this solver, are far more complicated and have only been dealt with in recent years. Notedly many of these analyses seem to have been using a primitive variable approach.

Chapter 3

Governing Equations and Methods of Computation

3.1 Flows of Incompressible Fluid

3.1.1 Overview

Real flows in the physical world are always compressible. That is to say, the density of the fluid medium in question is always varying in any particular field to a greater or lesser extent with respect to space and time. However, in many cases we can assume a 'mathematically perfect' flow in which the density of a particular field is constant in time and uniform in space. This is commonly called an 'incompressible flow'. These types of flow are an idealisation, and are not real. They form a subset of compressible flows. Ideally, we would try to solve the flow of a fluid medium that is in the low Mach number regime and therefore experiencing only small variations in density, with a compressible flow solver, fully accounting for this small variation. We can do this with a low Mach number correction. However, this is often inconveniently expensive to compute, with more equations to solve, and is susceptible to numerical instabilities. And, for example, as the speed of sound tends towards infinity in a compressible fluid flow the time step required in order to satisfy the CFL condition tends towards zero, increasing computational time. We desire then a set of *incompressible* fluid flow solvers which are efficient and accurate as a preferred alternative, and we want to continually develop these incompressible techniques so that they can help us advance science or advance engineering. This development is made more interesting by the fact that our scientific and technical developments are often running in parallel to rapid technological progress.

3.1.2 Approaches to the Solution

There exist six or seven primary classes or approaches to solving the incompressible Navier-Stokes' equation which have been developed over the years. In each method, there is a choice of strategy for discretisation including the finite element (FE), finite volume (FV), and finite difference (FD) approaches. Some examples of the primary classes include the SIMPLE algorithm (Semi-Implicit Method for Pressure-Linked Equations), Artificial Compressibility (AC), and Pressure-Projection (P-P) methods, which are ways to close the equations. Each approach has its own advantages, disadvantages, and features, which should be understood. The main approaches to numerical solution that have been developed are:

I . Pressure-Poisson

II . Artificial Compressibility

III . Pressure-Projection

IV . $\psi - \Omega$

V . $\vec{\psi} - \vec{\Omega}$

VI . FSAC-PP

VII . Pressure-Correction Methods

In any case, the major challenge of incompressible flow solvers is to satisfy the incompressible continuity equation (3.14), which contains the principle of conservation of mass. This is a difficult requirement for any incompressible fluid flow solver.

Essentially, we must understand the details of each approach; especially as each software package, whether Ansys Fluent, OpenFOAM, or Simcenter STAR-CCM+, will be using a different pressure-velocity coupling algorithm and implementing in their own way, which may lead to a different spatial evolution of the flow. We should know which approach the commercial software is using to ensure we capture the correct physics as efficiently as possible.

3.1.3 The Governing Equations

First we define the dimensionless *global* Mach number. This allows us to specify the broad flows for which the incompressible fluid assumption is valid. The Mach number

is case-specific, meaning it is not general because it depends upon the reference velocity chosen in each specific case.

$$Ma = \frac{u_c}{a} = \frac{u_\infty}{a} \tag{3.1}$$

This is global Mach number as opposed to local Mach number which gives a general characterisation of the fluid flow behaviour in the problem at hand. Here $u_c = u_\infty$ which is called the 'characteristic' or 'reference' velocity, and a is the speed of sound within that particular fluid medium. An interesting addition of complexity would be to consider a medium in which the speed of sound varies significantly. Most authors agree that when $Ma = 0.2$ or $Ma = 0.3$, we can consider the density to be constant without considerable error. In reality, Mach number varies locally for example flow may accelerate over an aerofoil causing an increase in speed and Mach number locally. Local Mach number variation may in some cases be significant enough to lead to compressible effects, in which case errors arising from the incompressible flow assumption may become more noticeable. In this case, there exists an option of combining incompressible and compressible solvers which is interesting. But provided that the global Mach number is less than 0.3 for our particular problem, we assume that

$$\rho(x,y,z;t) = constant \tag{3.2}$$

This is our foundational assumption.

This leads to several other observations. For example, if the density is constant, then it is no longer a function of pressure and *vice versa*. That is to say,

$$\rho \neq \rho(p) \tag{3.3}$$

and

$$p \neq p(\rho) \tag{3.4}$$

And the direct result of this is that our equation of state is no longer valid:

$$p \neq \rho RT \tag{3.5}$$

Therefore, we no longer have an independent equation for the pressure as we do in compressible flows and we need to find a new relationship between the velocity and pressure. This coupling is constructed mathematically, but it must also be physically true.

In light of the idealisation of equation 3.2 and its consequences, we can look again at the equations for the conservation of mass and momentum. In our context of Newtonian physics, we are using primarily the three fundamental laws of nature:

1. *Mass is conserved.*
2. *Momentum is conserved.*
3. *Energy is conserved.*

In any case, we can disregard energy conservation if we are not considering great variation in temperature.

The mass conservation principle is:

$$\frac{\partial \rho}{\partial t} + \nabla \cdot (\rho \vec{u}) \equiv \frac{\partial \rho}{\partial t} + div(\rho \vec{u}) = 0 \tag{3.6}$$

where we say

$$\rho = \rho(x, y, z; t) \tag{3.7}$$

$$\vec{u} = \vec{u}(x, y, z; t) = u\vec{e}_x + v\vec{e}_y + w\vec{e}_z \tag{3.8}$$

and,

$$\nabla = \left(\frac{\partial}{\partial x}\vec{e}_x + \frac{\partial}{\partial y}\vec{e}_y + \frac{\partial}{\partial z}\vec{e}_z \right) \tag{3.9}$$

The variables in equation 3.7 and 3.8 are known as the *primitive variables* as they are derived from integral calculus. In equation 3.8, the scalar components of the velocity vector are also a function of space and time in Cartesian coordinates,

$$u = u(x, y, z; t) \tag{3.10}$$

$$v = v(x, y, z; t) \tag{3.11}$$

$$w = w(x, y, z; t) \tag{3.12}$$

When we expand the conservation of mass equation 3.6 we get,

$$\frac{\partial \rho}{\partial t} + \rho(\nabla \cdot \vec{u}) + \vec{u}\,\nabla\rho \equiv \frac{\partial \rho}{\partial t} + \rho div(\vec{u}) + \vec{u}\,grad\rho = 0 \tag{3.13}$$

This is a mathematical description of the principle of conservation of mass for flows of compressible fluid. We also call this equation 'the continuity equation for flows of compressible fluid' or simply 'the continuity equation'. We see that when the nabla vector-type differential operator acts on a scalar we call the result 'the gradient' which is a vector. When the nabla vector-type operator acts on a vector we call the result 'the divergence' and it is a scalar product with a scalar result.

Considering that the density does not vary in space nor time, then the first and third terms in equation 3.13 disappear and this leaves,

$$\nabla \cdot \vec{u} = 0 \tag{3.14}$$

in vector form and,

$$\frac{\partial u}{\partial x} + \frac{\partial v}{\partial y} + \frac{\partial w}{\partial z} = 0 \tag{3.15}$$

in scalar form. We have divided both sides of the equation by the density which is scalar, constant, and uniform. This is the continuity equation for the flow of an incompressible fluid and is also called the 'divergence-free constraint' of the velocity field. Iteratively, our solver will meet this condition. Physically, this means that the volumetric expansion or contraction of each fluid element is zero. Each element may deform in the flow but its volume will not change.

As mentioned previously, this is a tough condition to meet for all classes of incompressible fluid flow solver. A good solver may have $\Delta\varepsilon = 10e-6$ or $10e-9$, where

$\rho_{solver} = \rho_{real} + \Delta\varepsilon$. That is to say, although we prescribed a zero value in the physical formulation, our numerical simulation will inevitably introduce errors.

In light of equation 3.14, we look again at the momentum equation which is a mathematical representation of the principle of conservation of momentum for a flow of compressible fluid. This is more commonly known as the compressible Navier-Stokes' equation:

$$\frac{\partial(\rho\vec{u})}{\partial t} + \nabla\cdot(\rho\vec{u}\otimes\vec{u}) = \rho\vec{g} - \nabla p + \mu\nabla^2\vec{u} + \frac{\mu}{3}\nabla(\nabla\cdot\vec{u}) \tag{3.16}$$

where $\vec{g} = \vec{g}(x,y,z;t) = g_x\vec{e}_x + g_y\vec{e}_y + g_z\vec{e}_z$ is the gravity vector field in Cartesian coordinates, μ is the constant dynamic viscosity, $p = p(x,y,z;t)$ is the scalar pressure field, ρ is the scalar density field, and $\vec{u}$ is the velocity vector field, as already defined.

We can divide by the scalar constant ρ, and get rid of the final term on the right hand side if we consider a fluid which is incompressible. That is, we assume that the divergence of velocity of the fluid is zero or that there is no expansion or contraction in volume of the continuum elements. This gives us,

$$\frac{\partial\vec{u}}{\partial t} + \nabla\cdot(\vec{u}\otimes\vec{u}) = \vec{g} - \frac{1}{\rho}\nabla p + \frac{\mu}{\rho}\nabla^2\vec{u} \tag{3.17}$$

This is Navier-Stokes' momentum equation for a flow of incompressible fluid. At times this can be more difficult to solve than the compressible Navier-Stokes' equation. Here, the left hand side represents the components of acceleration and the right hand side the forces per unit mass. The first term on the left hand side is the unsteady term, representing variation in the velocity vector field with time. The second term is the non-linear convective or advective term in conservative form, representing variation of the velocity vector field with space. This says that the act of motion of a fluid element will feed its own acceleration, which creates a self-feeding mechanism which is non-linear in character. This term is the cause of much trouble with Navier-Stokes' equation. The right hand side shows the effect of the scalar pressure force field per unit mass and the Laplacian term shows the viscous diffusion of momentum, or 'molecular diffusion'. The non-linear acceleration on the left hand side is tempered by the viscous term on the right hand side, and this is the basis of the non-dimensional Reynolds' number. As we can see, we have

no independent equation for p on the right hand side, we have time-dependence on the left hand side, and we also have to deal with the non-linear term $\nabla \cdot (\vec{u} \otimes \vec{u})$ on the left hand side. This is what makes finding an incompressible fluid flow solution particularly challenging.

Using the following vector identity, we can express the non-linear term in convective form,

$$\nabla \cdot (\vec{a} \otimes \vec{b}) = (\nabla \cdot \vec{a})\vec{b} + (\vec{b} \cdot \nabla)\vec{a} \tag{3.18}$$

Set $\vec{a} = \vec{b} = \vec{u}$,

$$\nabla \cdot (\vec{u} \otimes \vec{u}) = (\nabla \cdot \vec{u})\vec{u} + (\vec{u} \cdot \nabla)\vec{u} \tag{3.19}$$

For flows of incompressible fluid, using equation 3.14, the first term on the right hand side disappears,

$$\nabla \cdot (\vec{u} \otimes \vec{u}) = (\vec{u} \cdot \nabla)\vec{u} \tag{3.20}$$

These are two different forms of the same non-linear convective/advective term. The left hand side is the conservation form of the non-linear convective term and the right hand side is the convective form of the non-linear convective term. They are equivalent, but we may choose one or the other depending on our discretisation strategy. Knowing that discontinuities may arise at any time simply from the nature of the incompressible Navier-Stokes' equation, we may want to implement compressible flow techniques like Riemann solvers or high-order interpolation schemes, despite there being no shockwaves in the problems we are concerned with. In this case, the conservation form is preferable. For other strategies, like the SIMPLE algorithm, we have to use the convective form of the non-linear convective term.

It is important that we discretise the non-linear convective term correctly and accurately. Software like Fluent may linearise this term; this will lead to a loss of information. For example, certain details of vortical structures may be lost. On the other hand, the numerical scheme chosen may introduce error which *produces* false vortical structures or false physics, as opposed to losing information.

Summarising the governing equations for the flow of incompressible fluid, and using equation 3.20, we can write in vector form,

$$\boxed{\nabla \cdot \vec{u} = 0} \tag{3.21}$$

$$\boxed{\frac{\partial \vec{u}}{\partial t} + (\vec{u} \cdot \nabla)\vec{u} = \vec{g} - \frac{1}{\rho}\nabla p + \nu \nabla^2 \vec{u}} \tag{3.22}$$

Equation 3.21 is an elliptic equation and equation 3.22 is a parabolic equation; these behaviours interact so that we have a mixed elliptic-parabolic system. To fully describe the system, we would need to include the energy equation which includes the temperature. But this equation is not coupled with the continuity and momentum equations above, so it can be considered independently. Furthermore, we consider only problems where temperature is not varying significantly.

Equation 3.22 does not have an independent equation for the pressure field prediction. Our goal is to find the following fields:

$$p(x,y,z;t) = ? \tag{3.23}$$

$$u(x,y,z;t) = ? \tag{3.24}$$

$$v(x,y,z;t) = ? \tag{3.25}$$

$$w(x,y,z;t) = ? \tag{3.26}$$

We thus have four equations and four unknowns, and since we have no independent equation for pressure, we must construct mathematically a pressure-velocity coupling method. No analytical solution exists for the three dimensional incompressible flows and the solution has been searched for for over a hundred years. It is a Millenium Prize problem. Ladyshenskaya found a solution in two dimensions, and we have looked at

certain 1D solutions previously including Hagen-Poussieuille flow in a 2D channel.

Not only is the pressure-velocity coupling method required, there is also the problem of the non-linear term, and we also have time variation making the problem very complicated.

We write the governing equations in scalar form so that a computer can help us,

$$\frac{\partial u}{\partial x}+\frac{\partial v}{\partial y}+\frac{\partial w}{\partial z}=0 \tag{3.27}$$

The scalar momentum equation for velocity component x:

$$\frac{\partial u}{\partial t}+u\frac{\partial u}{\partial x}+v\frac{\partial u}{\partial y}+w\frac{\partial u}{\partial z}=g_x-\frac{1}{\rho}\frac{\partial p}{\partial x}+\nu\left(\frac{\partial^2 u}{\partial x^2}+\frac{\partial^2 u}{\partial y^2}+\frac{\partial^2 u}{\partial z^2}\right) \tag{3.28}$$

The scalar momentum equation for velocity component y:

$$\frac{\partial v}{\partial t}+u\frac{\partial v}{\partial x}+v\frac{\partial v}{\partial y}+w\frac{\partial v}{\partial z}=g_y-\frac{1}{\rho}\frac{\partial p}{\partial y}+\nu\left(\frac{\partial^2 v}{\partial x^2}+\frac{\partial^2 v}{\partial y^2}+\frac{\partial^2 v}{\partial z^2}\right) \tag{3.29}$$

The scalar momentum equation for velocity component z:

$$\frac{\partial w}{\partial t}+u\frac{\partial w}{\partial x}+v\frac{\partial w}{\partial y}+w\frac{\partial w}{\partial z}=g_z-\frac{1}{\rho}\frac{\partial p}{\partial z}+\nu\left(\frac{\partial^2 w}{\partial x^2}+\frac{\partial^2 w}{\partial y^2}+\frac{\partial^2 w}{\partial z^2}\right) \tag{3.30}$$

Any mathematical solution to these equations must also produce fields which are physically meaningful.

The continuity equation is not hyperbolic. If we would like to use characteristics, we would have to make the set of equations hyperbolic. Taking the divergence of the momentum equation will give us the pressure-Poisson which we can use for the pressure field and as a coupling method. We can also use the Helmholtz-Hodge decomposition, that is the fundamental theorem of vector analysis and tensor calculus, which says a vector field can always be decomposed into rotational and irrotational components. The scalar pressure field is irrotational and the velocity vector field is rotational - this is the basis of Chorin's pressure-projection method. Alternatively, we can also take the curl or rotation of the Navier-Stokes, deriving the vorticity formulations which use the vorticity transport equation which does not contain the pressure explicitly. It is this last approach which is

the subject of this thesis. These methods give us the velocity field, which we can then use to get the pressure field by the Bernoulli equation or the pressure-Poisson equation.

These approaches together cover all types of elliptic, parabolic, and hyperbolic partial differential equations between them. Furthermore, the non-linear term is present and difficult. And each method may also require different discretisation strategies, and has its own particular strengths and weaknesses. Also, we have to ensure that the pressure field we do produce is physically correct, and that our flow evolves correctly in space and time. We also have pseudo-time stepping methods available.

Fundamentally, we have four equations and four unknowns - u, v, w, p. In terms of our approach to solution, there are two frameworks to decide in any case, that is our choice of pressure-velocity coupling method and our discretisation strategy. In this thesis, we are concerned solely with vorticity formulations and the finite difference method.

Chapter 4

The $\psi - \Omega$ Formulation

This is the first of the so-called '*vorticity formulations*'. Historically, it was one of the most popular approaches to the solution of the flow of incompressible fluids in two dimensions and it remains so. The vorticity formulations rather beautifully describe the field of the fluid medium in terms of millions of little spirals. The flow of this fluid medium is described by how these spirals are deformed and transported. This motion is described by the vorticity transport equation, which is derived in section 4.1.2.

4.1 Derivation of the $\psi - \Omega$ Formulation

4.1.1 Vorticity and Velocity

There exists, at every point in the domain, an axis pointing in a similar or different direction, about which the flow rotates clockwise or anticlockwise with a certain strength as represented conceptually in figure 4.1. These axes are the directional component of the vorticity vector field, that is the unit vectors, and the strength of rotation is given by the magnitude of the vector. The direction of rotation is given by the sign. There is, then, a continuous field of rotation defined mathematically as

$$\vec{\Omega} = \vec{\Omega}(x, y, z; t) \tag{4.1}$$

which is a function of space and time. We note that for this reason we must be aware of capturing the correct *spatial and temporal* evolution of the flow field. We can also write,

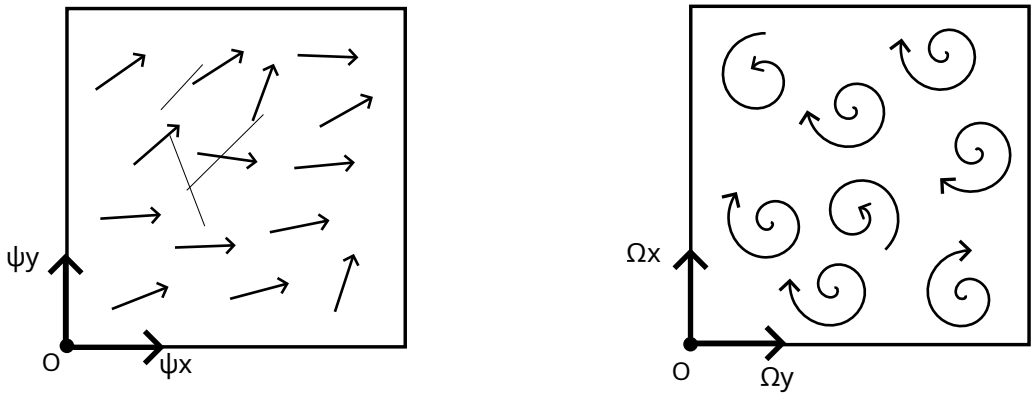

(a) Streamfunction, ψ (b) Vorticity, $\vec{\Omega}$

Figure 4.1: Conceptual drawing of ψ and $\vec{\Omega}$ in two dimensions

$$\vec{\Omega} = curl\,\vec{u} = rot\,\vec{u} \tag{4.2}$$

and,

$$\vec{\Omega} = \nabla \times \vec{u} \tag{4.3}$$

The vorticity vector field in two dimensions is represented conceptually in figure 4.1b. Expanding equation 4.3 the usual way when taking the cross product,

$$\left(\frac{\partial w}{\partial y} - \frac{\partial v}{\partial z}\right)\vec{e}_x + \left(\frac{\partial u}{\partial z} - \frac{\partial w}{\partial x}\right)\vec{e}_y + \left(\frac{\partial v}{\partial x} - \frac{\partial u}{\partial y}\right)\vec{e}_y = 0 \tag{4.4}$$

we can write the scalar components of the vorticity vector field,

$$\Omega_x = \frac{\partial w}{\partial y} - \frac{\partial v}{\partial z} \tag{4.5}$$

$$\Omega_y = \frac{\partial u}{\partial z} - \frac{\partial w}{\partial x} \tag{4.6}$$

$$\Omega_z = \frac{\partial v}{\partial x} - \frac{\partial u}{\partial y} \tag{4.7}$$

such that,

$$\vec{\Omega}(x,y,z;t) = \Omega_x \vec{e}_x + \Omega_y \vec{e}_y + \Omega_z \vec{e}_z \tag{4.8}$$

Here Ω_x, Ω_y, Ω_z are the scalar components of the vorticity vector which are also functions of space and time,

$$\Omega_x = \Omega_x(x,y,z;t) \tag{4.9}$$

$$\Omega_y = \Omega_y(x,y,z;t) \tag{4.10}$$

$$\Omega_y = \Omega_y(x,y,z;t) \tag{4.11}$$

From equation 4.4 - 4.7, we see that the vorticity field is dependent upon and defined by the vector velocity field components,

$$\vec{u} = u\vec{e}_x + v\vec{e}_y + w\vec{e}_z \tag{4.12}$$

Consider that in two dimensions there exists no z dimension, as demonstrated in figure 4.1. Therefore, $w = 0$ and any derivatives with respect to z are also zero. In light of this information, consider equations 4.5 - 4.7 again and we have,

$$\Omega_x = 0 \tag{4.13}$$

$$\Omega_y = 0 \tag{4.14}$$

$$\Omega_z = \frac{\partial v}{\partial x} - \frac{\partial u}{\partial y} \neq 0 \tag{4.15}$$

We find that only the z component of the vorticity vector remains in two dimensions.

Therefore the vorticity vector in two dimensions becomes,

$$\vec{\Omega} = \Omega_z \vec{e}_z = \left(\frac{\partial v}{\partial x} - \frac{\partial u}{\partial y} \right) \vec{e}_z \neq 0 \tag{4.16}$$

Which is to say, if one considers figure 6.1b, the rotation occuring about the x and y axes is zero everywhere in the field. Only the rotation tangential to the page is non-zero.

4.1.2 Derivation of the Equation for the Transport of Vorticity in Two Dimensions

We began with Navier-Stokes' momentum equation for a flow of incompressible fluid,

$$\frac{\partial \vec{u}}{\partial t} + (\vec{u} \cdot \nabla)\vec{u} = \vec{g} - \frac{1}{\rho}\nabla p + \nu \nabla^2 \vec{u} \tag{4.17}$$

We can replace the convective term using the following vector identity, where $\vec{a}$ is an arbitrary vector,

$$(\vec{a} \cdot \nabla)\vec{a} = \nabla \left(\frac{|\vec{a}|^2}{2} \right) - \vec{a} \times (\nabla \times \vec{a}) \tag{4.18}$$

and $|a|$ is the magnitude of the vector. Substituting $\vec{a} \equiv \vec{u}$, we get

$$(\vec{u} \cdot \nabla)\vec{u} = \nabla \left(\frac{|\vec{u}|^2}{2} \right) - \vec{u} \times (\nabla \times \vec{u}) \tag{4.19}$$

The second term on the right hand side of equation 4.19 includes the definition of the vorticity, as in equation 4.3. Hence,

$$(\vec{u}\cdot\nabla)\vec{u} = \nabla\left(\frac{|\vec{u}|^2}{2}\right) - \vec{u}\times\vec{\Omega} \tag{4.20}$$

Substituting this into Navier-Stokes' momentum equation for a flow of incompressible fluid, as repeated in equation 4.17, gives

$$\frac{\partial\vec{u}}{\partial t} - \vec{u}\times\vec{\Omega} = \vec{g} - \nabla\left(\frac{|\vec{u}|^2}{2}\right) - \frac{1}{\rho}\nabla p + \nu\nabla^2\vec{u} \tag{4.21}$$

The gravity field is conservative and irrotational (curl-free), so

$$\nabla\times\vec{g} \equiv curl\,\vec{g} \equiv rot\,\vec{g} = 0 \tag{4.22}$$

This implies that a scalar potential of the gravity field exists,

$$\vec{g} = -\nabla\Phi \equiv -grad\,\Phi \tag{4.23}$$

Substituting into equation 4.21,

$$\frac{\partial\vec{u}}{\partial t} - \vec{u}\times\vec{\Omega} = -\nabla\Phi - \nabla\left(\frac{|\vec{u}|^2}{2}\right) - \frac{1}{\rho}\nabla p + \nu\nabla^2\vec{u} \tag{4.24}$$

Which when rearranged becomes,

$$\frac{\partial\vec{u}}{\partial t} - \vec{u}\times\vec{\Omega} = -\nabla\left(\Phi - \frac{|\vec{u}|^2}{2} - \frac{p}{\rho}\right) + \nu\nabla^2\vec{u} \tag{4.25}$$

Here, from the first term on the right hand side, we can define the scalar function Π which is the total potential of mechanical energy,

$$\Pi = \Phi + \frac{|\vec{u}|^2}{2} + \frac{p}{\rho} \tag{4.26}$$

$$\frac{\partial \vec{u}}{\partial t} - \vec{u} \times \vec{\Omega} = -\nabla \Pi + \nu \nabla^2 \vec{u} \tag{4.27}$$

We now perform the critical step which is to take the curl of this Navier-Stokes momentum equation in rearranged form to get the vorticity transport equation,

$$\nabla \times \left[\frac{\partial \vec{u}}{\partial t} - \vec{u} \times \vec{\Omega} = -\nabla \Pi + \nu \nabla^2 \vec{u} \right] \tag{4.28}$$

$$\frac{\partial (\nabla \times \vec{u})}{\partial t} - \nabla \times (\vec{u} \times \vec{\Omega}) = -\nabla \times (\nabla \Pi) + \nu \nabla^2 (\nabla \times \vec{u}) \tag{4.29}$$

Here we make use of the vector identity,

$$\nabla \times (\nabla \phi) = 0 \tag{4.30}$$

to eliminate the first term on the right hand side. This leaves,

$$\frac{\partial \vec{\Omega}}{\partial t} - \nabla \times (\vec{u} \times \vec{\Omega}) = \nu \nabla^2 \vec{\Omega} \tag{4.31}$$

which is the first form of the *vorticity transport equation* that we encounter.

There exists a vector identity which we can use to expand the second term on the left hand side,

$$\nabla \times (\vec{a} \times \vec{b}) = \vec{a}(\nabla \cdot \vec{b}) - \vec{b}(\nabla \cdot \vec{a}) + (\vec{b} \cdot \nabla)\vec{a} - (\vec{a} \cdot \nabla)\vec{b} \tag{4.32}$$

Which, if we let $\vec{a} \equiv \vec{u}$ and $\vec{b} \equiv \vec{\Omega}$ becomes,

$$\nabla \times (\vec{u} \times \vec{\Omega}) = \vec{u}(\nabla \cdot \vec{\Omega}) - \vec{\Omega}(\nabla \cdot \vec{u}) + (\vec{\Omega} \cdot \nabla)\vec{u} - (\vec{u} \cdot \nabla)\vec{\Omega} \tag{4.33}$$

Substituting into equation 4.31,

$$\frac{\partial \vec{\Omega}}{\partial t} - \vec{u}(\nabla \cdot \vec{\Omega}) - \vec{\Omega}(\nabla \cdot \vec{u}) + (\vec{\Omega} \cdot \nabla)\vec{u} - (\vec{u} \cdot \nabla)\vec{\Omega} = \nu \nabla^2 \vec{\Omega} \tag{4.34}$$

Using the continuity equation for incompressible flows which results from our critical assumption of constant density, that is

$$\nabla \cdot \vec{u} = 0 \tag{4.35}$$

then it is clear that the third term on the left hand side will disappear. We also make use of another important vector identity,

$$\nabla \cdot (\nabla \times \vec{a}) = 0 \tag{4.36}$$

letting $\vec{a} \equiv \vec{u}$ so that,

$$\nabla \cdot (\nabla \times \vec{u}) = 0 \tag{4.37}$$

If we recall that the vorticity vector field is defined as,

$$\vec{\Omega} = \nabla \times \vec{u} \tag{4.38}$$

then substituting this into equation 4.39 gives,

$$\nabla \cdot \vec{\Omega} = 0 \tag{4.39}$$

which is to say, the divergence of vorticity is zero for the flow of an incompressible fluid.

Using equation 4.35 and 4.39 and substituting these into the second and third term of the left hand side of equation 4.34, which is a complicated form of the vorticity transport equation, we get

$$\boxed{\frac{\partial \vec{\Omega}}{\partial t} + (\vec{u} \cdot \nabla)\vec{\Omega} - (\vec{\Omega} \cdot \nabla)\vec{u} = \nu \nabla^2 \vec{\Omega}} \tag{4.40}$$

This is the ***equation for the transport of vorticity in three dimensions***.

On the left hand side, the first term is the term for the unsteadiness of the vorticity

vector field, the second is the term for non-linear convection/advection of vortices, and the third term is the term for the stretching of vortices. The term for the stretching of vortices only appears for three dimensional flows. On the right hand side, we have the term for the diffusion of vorticity. This makes up the transport equation for vorticity in three dimensions.

We used two important criteria in the derivation of the above equation, which arose from the constant density condition for incompressible fluid flows, these are:

1. *The divergence of velocity vector field is zero*
2. *The divergence of vorticity vector field is zero*

The extent to which we can satisfy these criteria indicates the effectiveness of our numerical method.

We can combine the first two terms on the left hand side using the definition of the material derivative, which leaves

$$\frac{D\vec{\Omega}}{Dt} = (\vec{\Omega}\cdot\nabla)\vec{u} + \nu\nabla^2\vec{\Omega} \tag{4.41}$$

Recalling earlier where we defined the vorticity vector field in two dimensions, and saw that only the z component remains, we can write $\vec{\Omega} = \Omega_z\vec{e}_z$, which leaves

$$\boxed{\frac{\partial\Omega_z}{\partial t} + (\vec{u}\cdot\nabla)\Omega_z = \nu\nabla^2\Omega_z} \tag{4.42}$$

This is the ***vector form of the equation for the transport of vorticity in two dimensions***. This is a parabolic PDE.

In scalar form, which is more suitable for discretisation,

$$\boxed{\frac{\partial\Omega_z}{\partial t} + u\frac{\partial\Omega_z}{\partial x} + v\frac{\partial\Omega_z}{\partial y} = \nu\left(\frac{\partial^2\Omega_z}{\partial x^2} + \frac{\partial^2\Omega_z}{\partial y^2}\right)} \tag{4.43}$$

where $\Omega_z = \frac{\partial v}{\partial x} - \frac{\partial u}{\partial y}$.

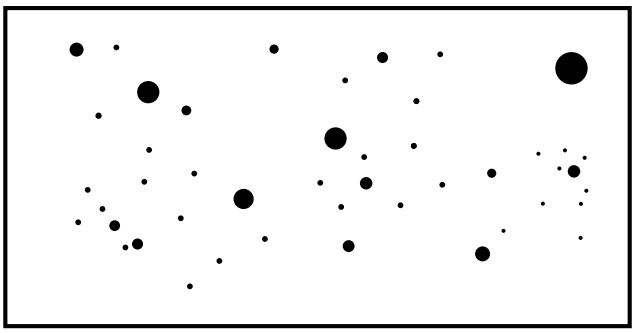

Figure 4.2: Conceptual drawing of an arbitrary scalar field in two dimensions. For example, the scalar field of the streamfunction, $\psi = \psi(x,y;t)$, which only exists in two dimensions. The size of the dot represents the magnitude of the scalar.

4.1.3 Streamlines for 2D Flows

In two dimensions, there exists a scalar function which when taking the derivative thereof with respect to y and with respect to x, gives the scalar components of the two dimensional velocity vector field. That is,

$$\boxed{u = \frac{\partial \psi}{\partial y}} \tag{4.44}$$

$$\boxed{v = -\frac{\partial \psi}{\partial x}} \tag{4.45}$$

which are also scalar fields, such that $\psi = \psi(x,y;t)$, $u = u(x,y;t)$, $v = v(x,y;t)$. Substituting these results into the divergence-free velocity constraint and we have,

$$\nabla \cdot \vec{u} = \frac{\partial u}{\partial x} + \frac{\partial v}{\partial y} = \frac{\partial}{\partial x}\left(\frac{\partial \psi}{\partial y}\right) + \frac{\partial}{\partial y}\left(-\frac{\partial \psi}{\partial x}\right) = \frac{\partial^2 \psi}{\partial x \partial y} - \frac{\partial^2 \psi}{\partial y \partial x} \tag{4.46}$$

If we then consider Schwarz's theorem,

$$\frac{\partial^2 \psi}{\partial x \partial y} = \frac{\partial^2 \psi}{\partial y \partial x} \tag{4.47}$$

this means,

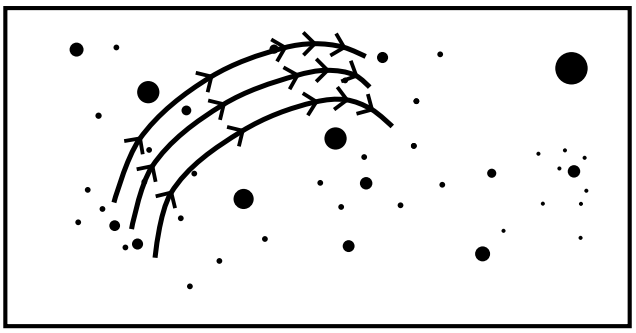

Figure 4.3: Conceptual drawing of the streamlines which are parallel to the velocity vectors which arise from the scalar field of the streamfunction

$$\nabla \cdot \vec{u} = \frac{\partial^2 \psi}{\partial x \partial y} - \frac{\partial^2 \psi}{\partial y \partial x} = 0 \tag{4.48}$$

implying that the streamfunction by way of its nature satisfies the divergence-free constraint on the velocity field. Hence the streamfunction is compatible with our incompressible fluid methodology.

If we combine equation 4.44 and 4.45 we get the velocity vector field,

$$\vec{u}(x,y;t) = u(x,y;t)\,\vec{e}_x + v(x,y;t)\,\vec{e}_y \tag{4.49}$$

From this velocity vector field arise the streamlines which are at every point parallel to the local velocity vector.

4.1.4 The Formulation

Consider again the two dimensional vorticity transport equation in scalar form,

$$\frac{\partial \Omega_z}{\partial t} + u\frac{\partial \Omega_z}{\partial x} + v\frac{\partial \Omega_z}{\partial y} = \nu\left(\frac{\partial^2 \Omega_z}{\partial x^2} + \frac{\partial^2 \Omega_z}{\partial y^2}\right) \tag{4.50}$$

We want to establish a relationship between the streamfunction and vorticity. Using equation 4.50, we can substitute equations 4.44 and 4.45, which gives

$$\boxed{\frac{\partial \Omega_z}{\partial t} + \frac{\partial \psi}{\partial y}\frac{\partial \Omega_z}{\partial x} - \frac{\partial \psi}{\partial x}\frac{\partial \Omega_z}{\partial y} = \nu\left(\frac{\partial^2 \Omega_z}{\partial x^2} + \frac{\partial^2 \Omega_z}{\partial y^2}\right)} \tag{4.51}$$

As written earlier, this is called the ***equation for the transport of vorticity in 2D and in scalar form***; this time it is written in terms of the streamfunction scalar field, ψ. This is a parabolic PDE.

To find a second relationship relating ψ and Ω, we can use the definition of the vorticity and substitute the definition of the streamfunction, which becomes

$$\Omega_z = \frac{\partial v}{\partial x} - \frac{\partial u}{\partial y} = \frac{\partial}{\partial x}\left(-\frac{\partial \psi}{\partial x}\right) - \frac{\partial}{\partial y}\left(\frac{\partial \psi}{\partial y}\right) = -\left(\frac{\partial^2 \psi}{\partial x^2} + \frac{\partial^2 \psi}{\partial y^2}\right) = -\nabla^2 \psi \tag{4.52}$$

Or,

$$\boxed{\frac{\partial^2 \psi}{\partial x^2} + \frac{\partial^2 \psi}{\partial y^2} = -\Omega_z(x,y;t)} \tag{4.53}$$

which is called the ***Poisson equation for the streamfunction in scalar form and in two dimensions***. This is an elliptic PDE.

These two equations, together with equations 4.44 and 4.45 are the heart of the streamfunction-vorticity formulation. The change of variables has allowed us to switch from a mixed elliptic-parabolic system of equations to a separate parabolic and elliptic equation. We can now describe the algorithm for solving the flow of incompressible fluids:

I . Solve the streamfunction-Poisson equation for ψ using a Poisson solver

II . Solve for the velocity field using finite differences of equations 4.44 and 4.45

III . Solve the 2D vorticity transport equation for Ω_z

IV . Solve the pressure-Poisson equation for the pressure field

4.2 Boundary Conditions

The boundary conditions for ψ and Ω_z as required to be set during the time-marching procedure are here derived according to Anderson *et al.* [12].

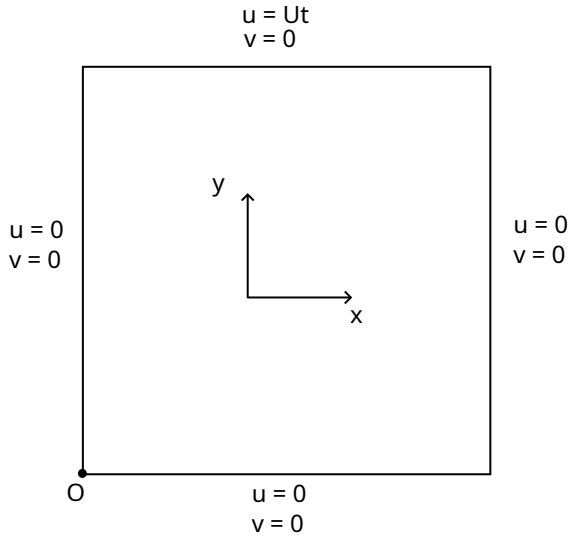

Figure 4.4: Two dimensional lid-driven cavity boundary conditions

Assuming rigid walls for a two dimensional cavity, we use the impermeability and no-slip conditions to define the velocity on each boundary, as in figure 4.4. To approach numerical solution, we require some conditions to restrain the flow development and contain the spatial and temporal evolution; that is we need boundary conditions for the velocity components, the streamfunction, and the vorticity. We need to know for certain at least some information about the flowfield if we can hope to find a solution for the rest of the domain. As stated by Anderson *et al.*, 'specification of boundary conditions is extremely important since it directly affects the stability and accuracy of the solution'. Looking at figure 4.4, we can see that in the top corners there will be a point where $u = Ut$ and $u = 0$ at the same point. This is a discontinuity which can cause difficulties. Furthermore, we know that ψ is constant on the wall, and as such it is usually set to zero. This means that the wall is acting like a streamline, that is there exists no normal component of velocity, and only the tangential components survive. This is a consequence of the impermeability condition for a solid rigid wall. In this case, the tangential components of velocity are also zero on the walls due to the no-slip condition, except for the top wall where motion is prescribed.

For the following prescriptions, we will use the same notation to index the node points as that used in the referenced Python code, that is $i = 0 : nx - 1$ and $j = 0 : ny - 1$, given that Python is zero-indexed. Here nx and ny are the number of nodes in the x and y directions respectively, and i and j are the indices for these nodes in these directions. This means that there are $nx - 1$ spaces in the x direction and $ny - 1$ spaces in the y direction.

Consider that we treat the wall as a streamline due to the impermeability condition, then *on the wall*,

$$\psi = C \tag{4.54}$$

where C is an arbitrary constant. We allow $C = 0$, so that on the wall,

$$\psi = 0 \tag{4.55}$$

and hence we have our boundary condition for ψ.

To derive the vorticity boundary conditions (using Anderson *et al.* [12]), consider first the left wall of the cavity in figure 4.4 with the origin defined at the bottom left corner. Use a Taylor series expansion for the value of ψ one step away from the wall using values of ψ and its derivatives at the wall,

$$\psi_{1,j} = \psi_{0,j} + \left.\frac{\partial \psi}{\partial x}\right|_{0,j} \Delta x + \frac{1}{2}\left.\frac{\partial^2 \psi}{\partial x^2}\right|_{0,j} (\Delta x)^2 + \frac{1}{3!}\left.\frac{\partial^3 \psi}{\partial x^3}\right|_{0,j} (\Delta x)^3 + \ldots \tag{4.56}$$

Using the prescribed velocity which results from the impermeability condition,

$$v = -\frac{\partial \psi}{\partial x} = 0 \tag{4.57}$$

Substitute this into equation 4.56, and rearrange for the second order term,

$$\frac{\partial^2 \psi}{\partial x^2} = \frac{2(\psi_{i,1} - \psi_{i,0})}{(\Delta x)^2} + O(\Delta x) \tag{4.58}$$

Recall,

$$\frac{\partial^2 \psi}{\partial x^2} + \frac{\partial^2 \psi}{\partial y^2} = -\Omega_z(x, y; t) \tag{4.59}$$

On the left wall, ψ is constant in the y direction, so

$$\frac{\partial^2 \psi}{\partial x^2} = -\Omega_z(x,y;t) \tag{4.60}$$

Substitute this into equation 4.58 and we have the boundary condition for the vorticity on the left wall for all t,

$$\Omega_{z,0,j} = \frac{2(\psi_{0,j} - \psi_{1,j})}{(\Delta x)^2} + O(\Delta x) \tag{4.61}$$

A similar process can be used for the right and bottom walls. Given that ψ is constant and $\psi = 0$ on the walls,

$$\psi_{wall} \equiv \psi_{0,j} \equiv \psi_{nx-1,j} \equiv \psi_{i,0} \equiv \psi_{i,ny-1} = 0 \tag{4.62}$$

So that our boundary conditions are,

$$\Omega_{z,0,j} = \frac{2(\psi_{wall} - \psi_{1,j})}{(\Delta x)^2} + O(\Delta x) \tag{4.63}$$

$$\Omega_{z,nx-1,j} = \frac{2(\psi_{wall} - \psi_{1,j})}{(\Delta x)^2} + O(\Delta x) \tag{4.64}$$

$$\Omega_{z,i,0} = \frac{2(\psi_{wall} - \psi_{i,1})}{(\Delta x)^2} + O(\Delta x) \tag{4.65}$$

for the left, right, and bottom walls respectively.

There is a slight discrepancy for the top wall, because the x component of velocity is not zero. Consider the Taylor series expansion of ψ to one step below the top wall using the value of ψ and its derivatives at the wall,

$$\psi_{i,ny-2} = \psi_{i,ny-1} - \left.\frac{\partial \psi}{\partial x}\right|_{i,ny-1} \Delta x + \frac{1}{2}\left.\frac{\partial^2 \psi}{\partial x^2}\right|_{i,ny-1} (\Delta x)^2 - \frac{1}{3!}\left.\frac{\partial^3 \psi}{\partial x^3}\right|_{i,ny-1} (\Delta x)^3 + \ldots \tag{4.66}$$

and recall that,

$$u_{i,ny-1} = \left.\frac{\partial \psi}{\partial x}\right|_{i,ny-1} \tag{4.67}$$

Substituting equation 4.67 into equation 4.66, and rearranging for the second order derivative, gives,

$$\left.\frac{\partial^2 \psi}{\partial y^2}\right|_{i,ny-1} = \frac{2\left(\psi_{i,ny-2} - \psi_{i,ny-1} + u_{i,ny-1}\Delta y\right)}{(\Delta y)^2} + O(\Delta y) \tag{4.68}$$

Recalling again equation 4.59, and that ψ is constant on the top wall in the x direction, then substituting and rearranging gives,

$$\Omega_{z,i,ny-1} = \frac{2(\psi_{wall} - \psi_{i,ny-2})}{(\Delta y)^2} - \frac{2u_{i,ny-1}}{\Delta y} \tag{4.69}$$

This is the equation for the vorticity on the top wall. Equations 4.63, 4.64, 4.65, together with equation 4.55 constitute the boundary conditions for the $\psi - \Omega$ method in a two dimensional cavity.

4.3 Link to the Code

The following is a link to the public GitHub repository housing the code corresponding to this section. The streamfunction-vorticity formulation code can be found under the directory name '*psi_omega*'. Please read the '*README.md*' file for further details about the repository:

`https://github.com/abrierley0/incompressible_repo/tree/main`

Chapter 5

The Lid-Driven Cavity in Two Dimensions

The square cavity problem contains within it the whole universe of fluid mechanics, as a problem containing information about the nature of fluid motion and structures. For example, it contains Taylor's scraper problem, Moffat eddies, the Prandtl-Batchelor theorem, and encapsulates the inherent nature of the Navier-Stokes' equation. This information has been extracted experimentally, numerically, and analytically over the course of centuries and is still incomplete. Yet it is a well-studied benchmark against which to validate when developing new solvers. Here the $\psi - \Omega$ formulation was written as a preliminary step for the more complicated three dimensional $\vec{\psi} - \vec{\Omega}$ formulation.

The results from the code for the flow of an incompressible fluid medium under the shear stress of a driving lid in a contained two dimensional square cavity, using the well-studied streamfunction-vorticity formulation, are shown.

In each case, comparison of results have been drawn with early formulations, such as Kawaguti and Burggraf's work. There are visual comparisons as well as more reliable validation using the centreline velocity.

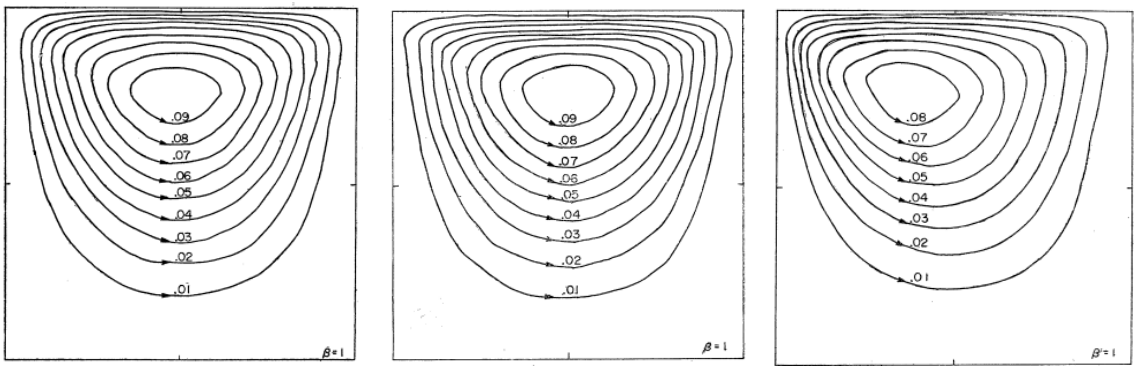

(a) Re = 0 (b) Re = 8 (c) Re = 64

Figure 5.1: The results of Kawaguti [1]

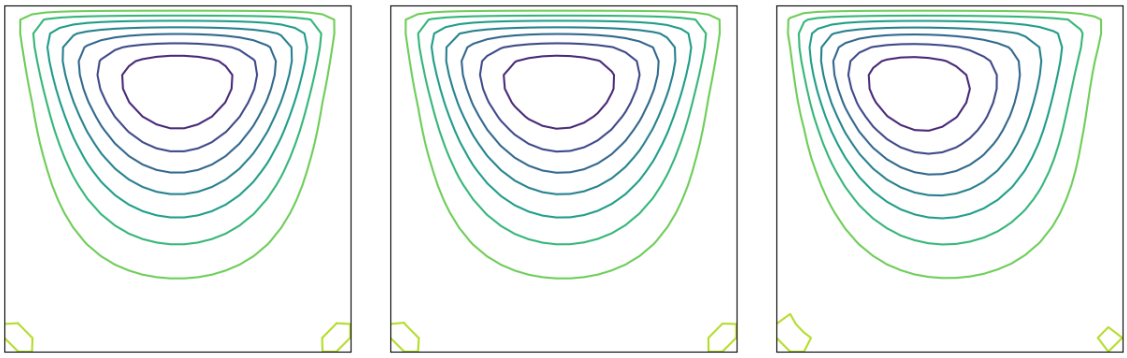

(a) Re = 0 (b) Re = 8 (c) Re = 64

Figure 5.2: My results

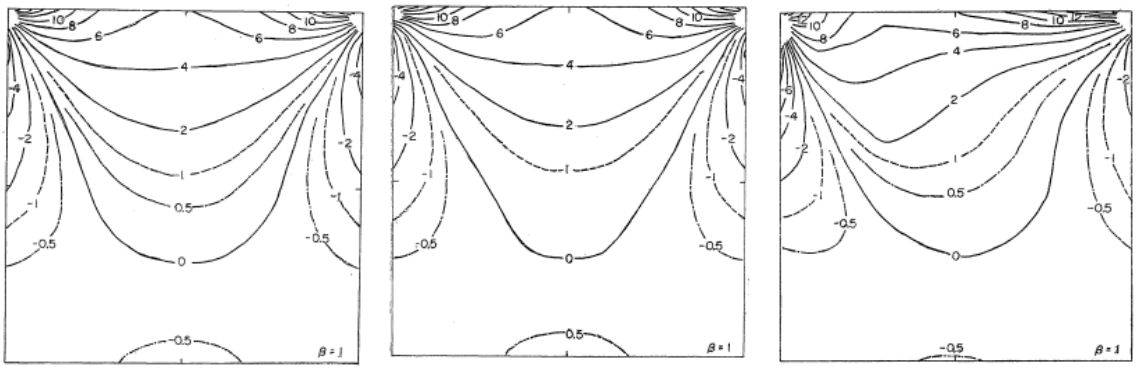

(a) Re = 0 (b) Re = 8 (c) Re = 64

Figure 5.3: Vorticity contours of Kawaguti

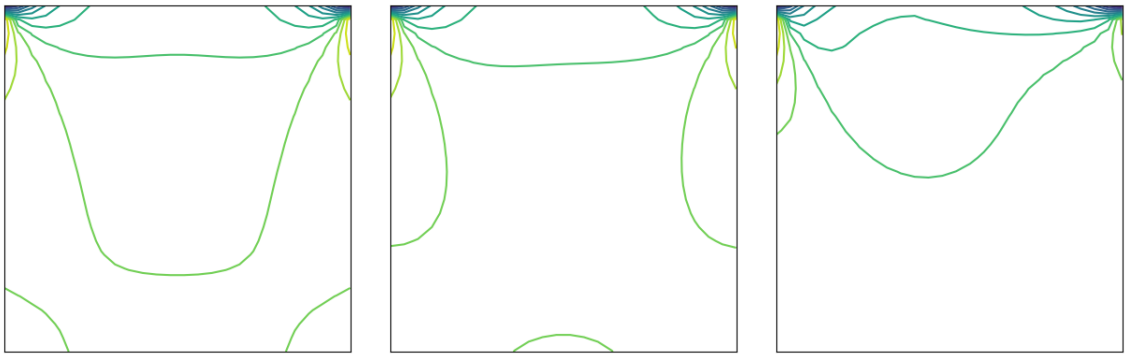

(a) Re = 0 (b) Re = 8 (c) Re = 64

Figure 5.4: My vorticity contours

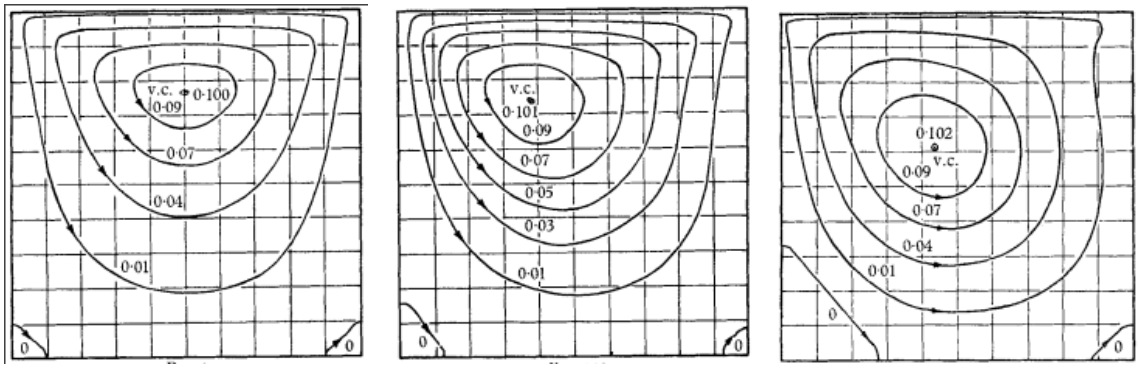

(a) Re = 0 (b) Re = 100 (c) Re = 400

Figure 5.5: The streamlines of Burggraf [2]

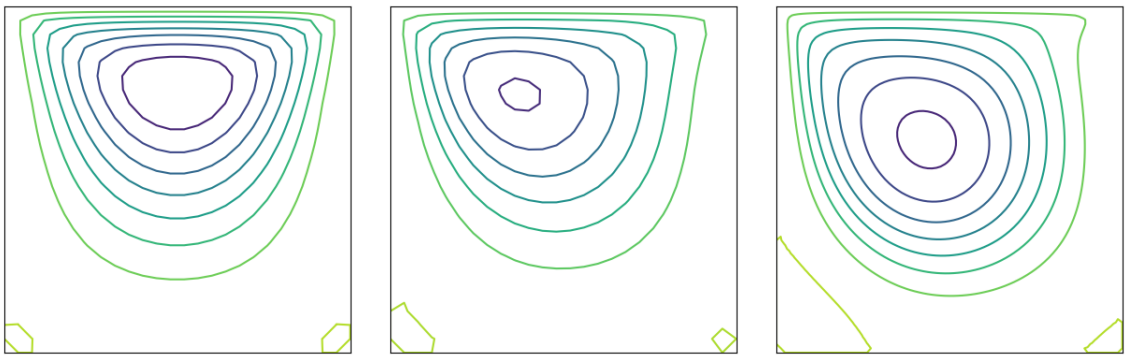

(a) Re = 0 (b) Re = 100 (c) Re = 400

Figure 5.6: My streamlines

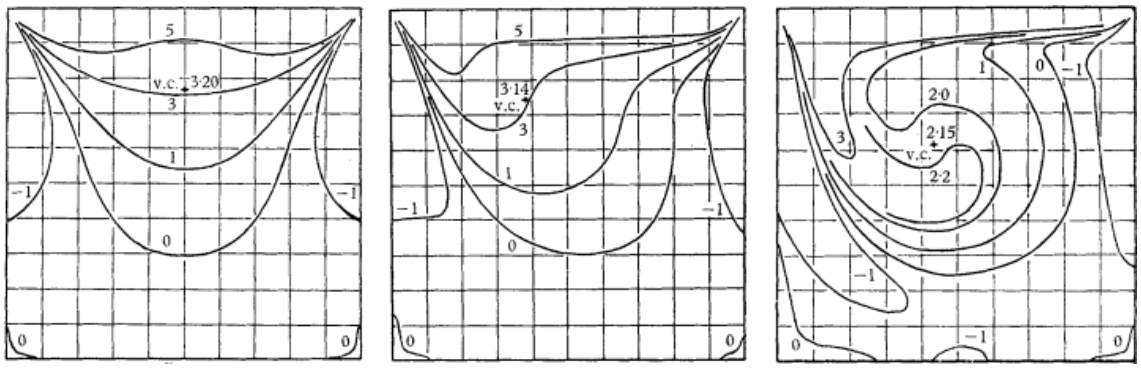

(a) Re = 0 (b) Re = 100 (c) Re = 400

Figure 5.7: The vorticity contours of Burggraf [2]

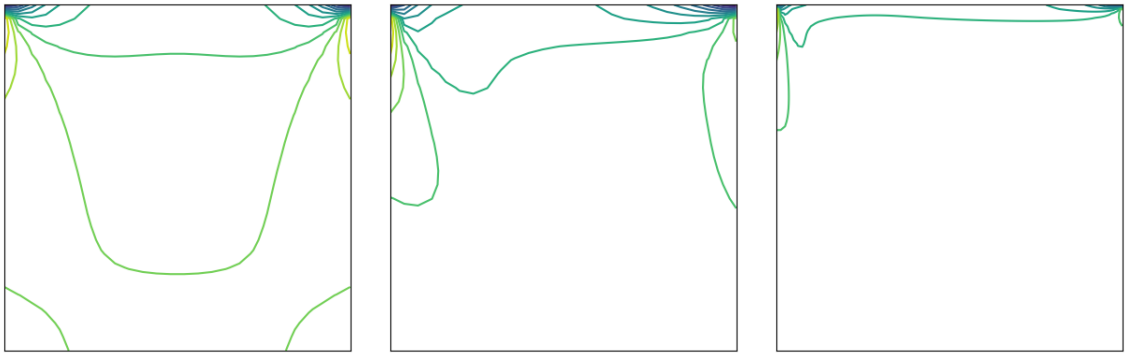

(a) Re = 0 (b) Re = 100 (c) Re = 400

Figure 5.8: My vorticity contours

Poisson parameters for Re=0 and Re=100 were: beta = 1.5 tol = 1e-4 maxIt = 30.

The discontinuous contour plot is shown rather than the smooth plot to emphasise that we are using a discrete *numerical* approximation of the truth, albeit a good one

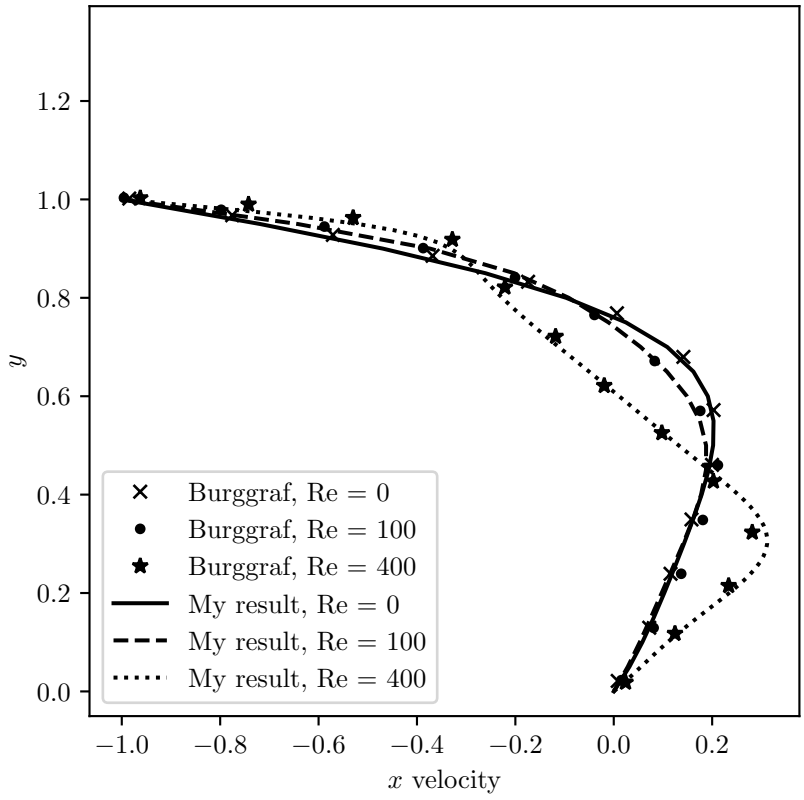

Figure 5.9: x velocity along the centreline, lid motion is right to left

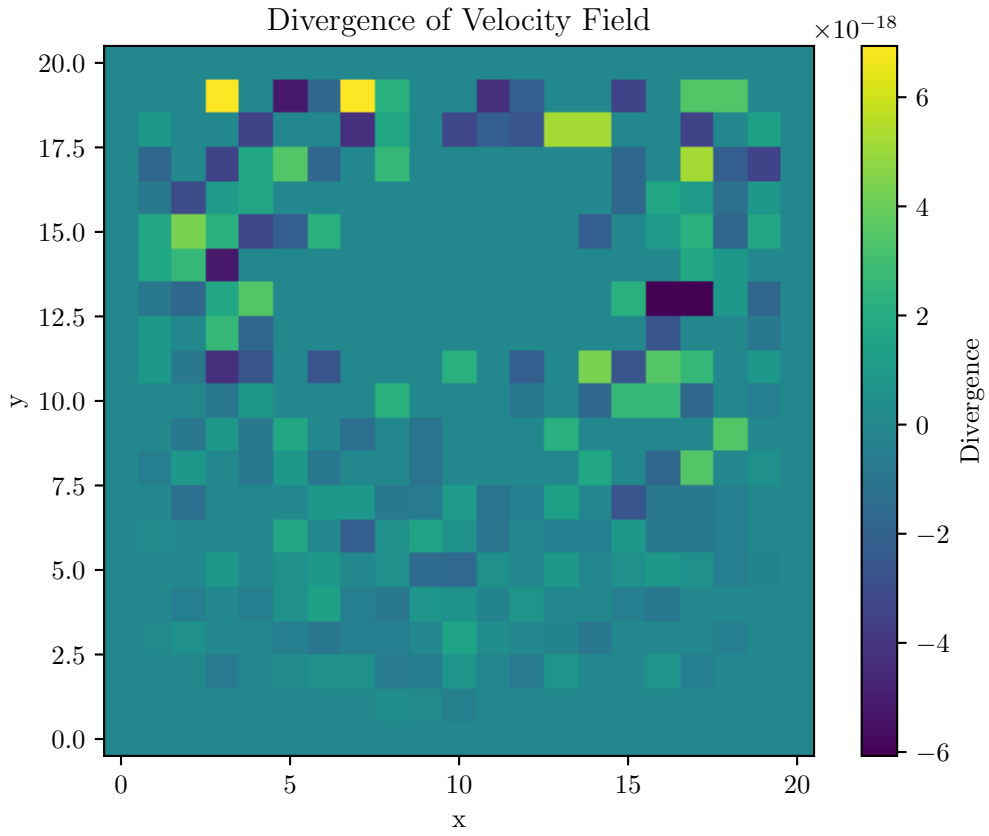

Figure 5.10: Divergence of velocity for the $\psi - \Omega$ formulation in two dimensions for Re = 0 with grid = 21^2

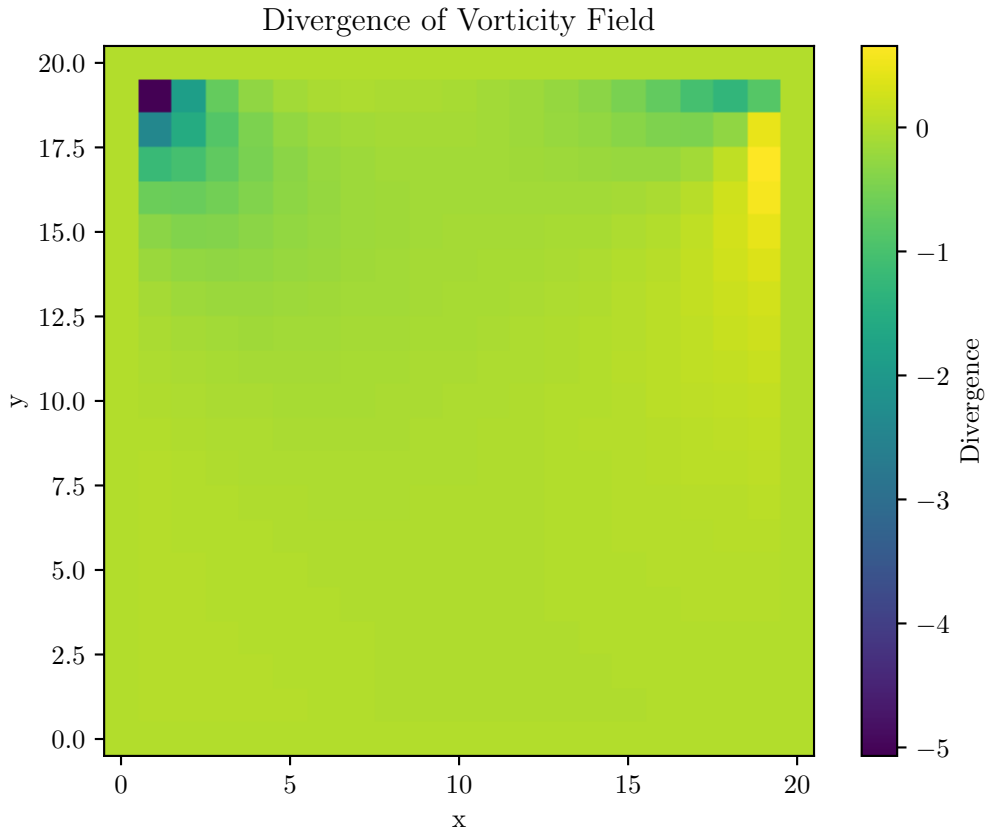

Figure 5.11: Divergence of vorticity for the $\psi - \Omega$ formulation in two dimensions for Re = 0 with grid = 21^2

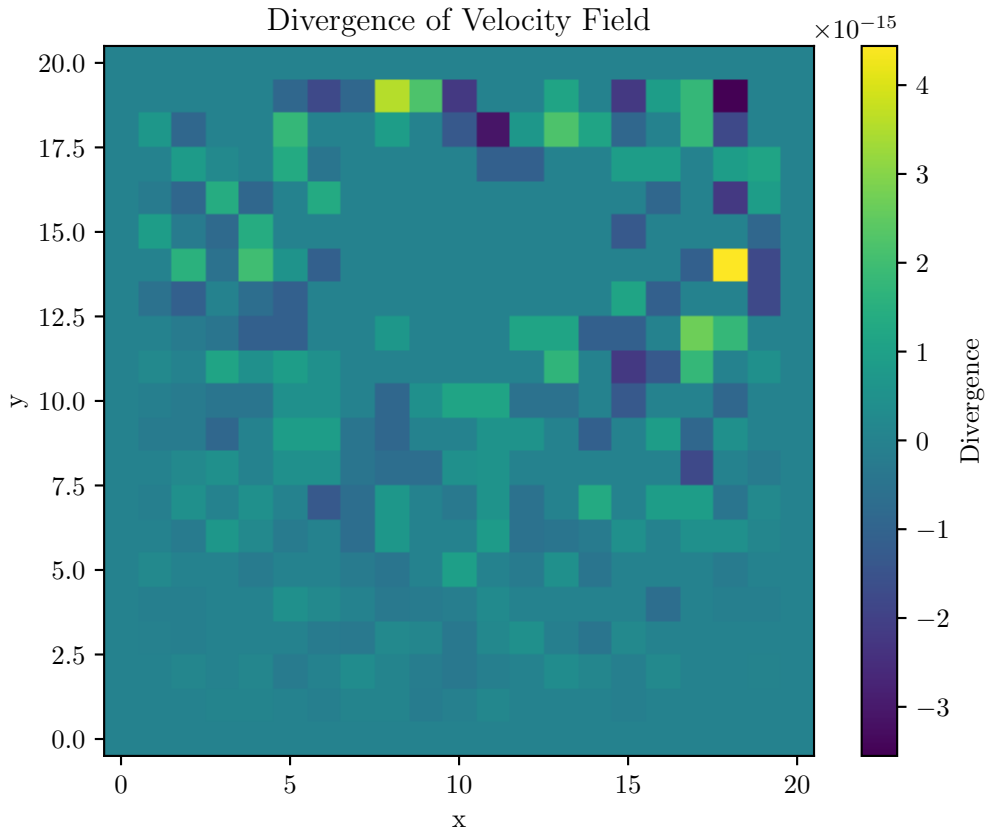

Figure 5.12: Divergence of velocity for the $\psi - \Omega$ formulation in two dimensions for Re = 100 with grid = 21^2

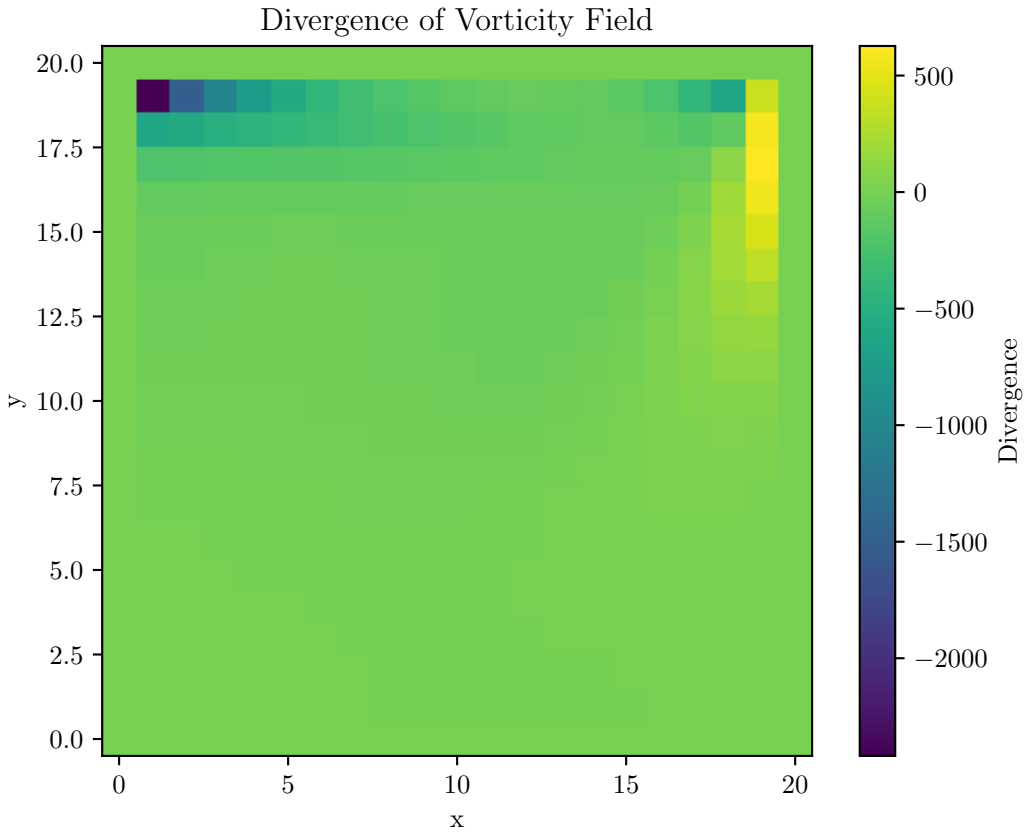

Figure 5.13: Divergence of vorticity for the $\psi - \Omega$ formulation in two dimensions for Re = 100 with grid = 21^2

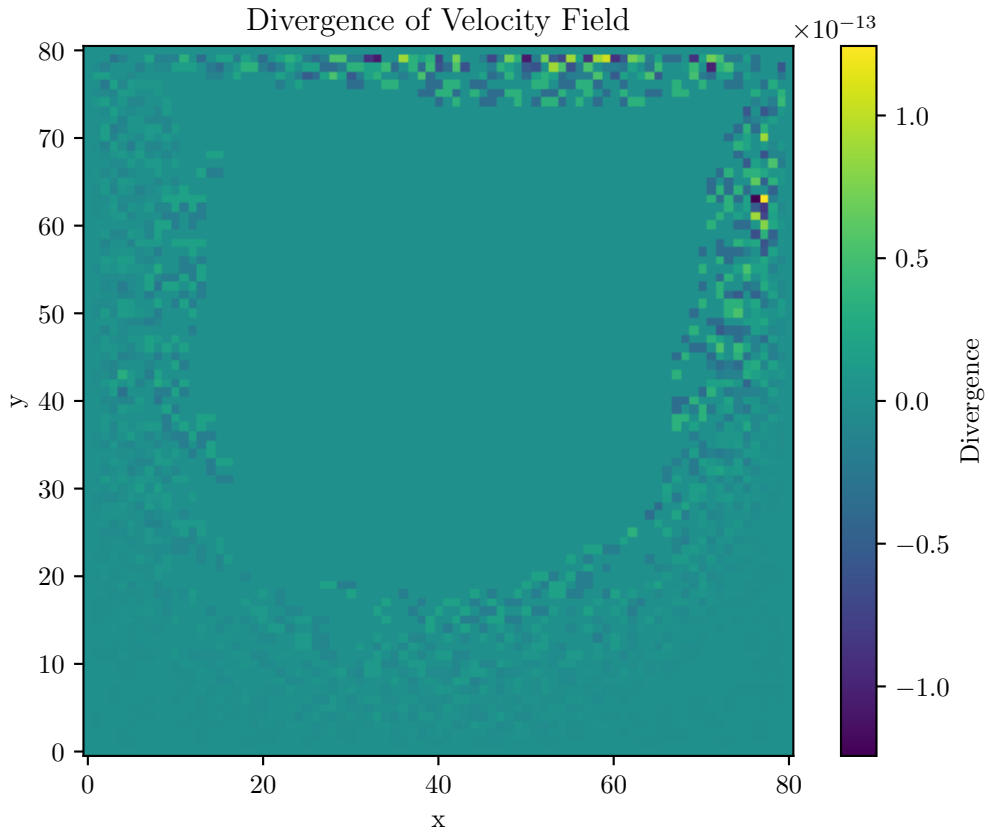

Figure 5.14: Divergence of velocity for the $\psi - \Omega$ formulation in two dimensions for Re = 400 with grid = 81^2

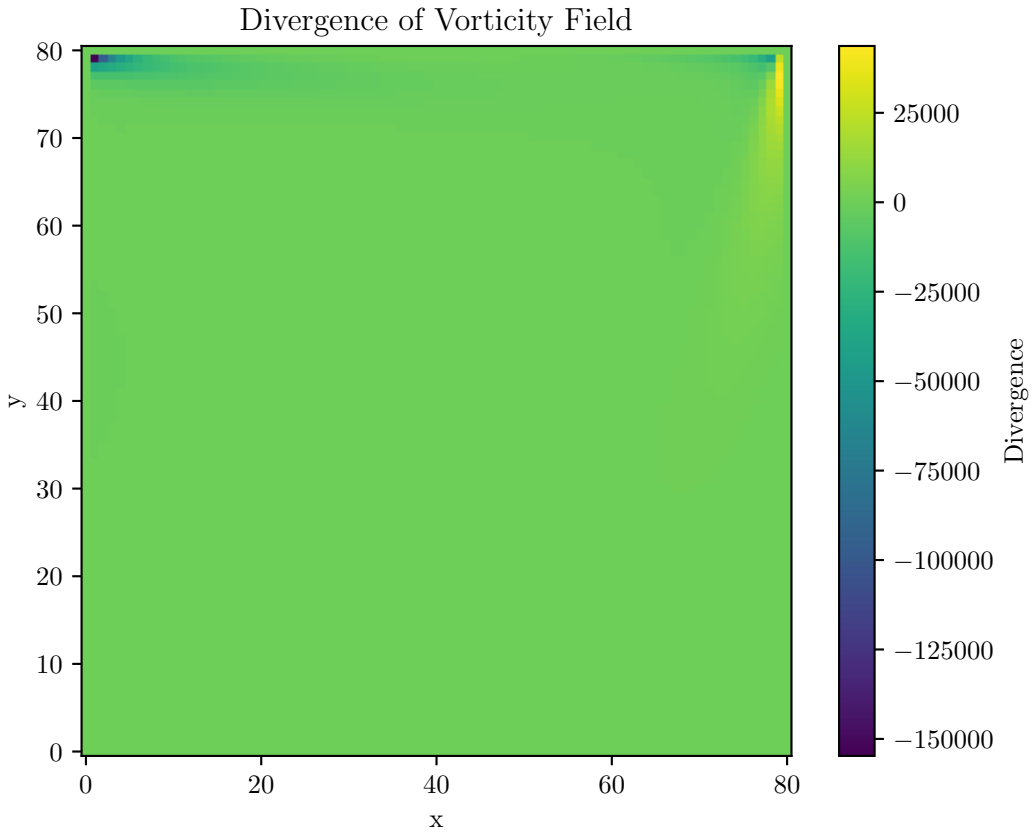

Figure 5.15: Divergence of vorticity for the $\psi - \Omega$ formulation in two dimensions for Re = 400 with grid = 81^2

Chapter 6

The $\vec{\psi} - \vec{\Omega}$ Formulation

The second of the vorticity-based formulations is the $\vec{\psi} - \vec{\Omega}$ formulation. This is a three dimensional analogue of the $\psi - \Omega$ formulation previously covered, where the streamfunction has been replaced by the vector potential. This formulation is the main subject of this thesis.

6.1 The Governing Equations

In two dimensions, the streamfunction exists. This is not the case in three dimensions. Furthermore, recall that two of the vorticity components disappeared in the two dimensional case; in the three dimensional case this is no longer so. The flow is fully vortical and rotational in three dimensions,

$$\vec{\Omega} = \vec{\Omega}(x,y,z;t) = \Omega_x \vec{e}_x + \Omega_y \vec{e}_y + \Omega_z \vec{e}_z = \nabla \times \vec{u} \neq \vec{0} \tag{6.1}$$

A conceptual visualisation of three dimension vorticity field is shown in figure 6.1b. There is essentially a field of unit vectors about which local flow rotates with a certain magnitude and direction. This is what the equation 6.1 describes.

As well as the vorticity in three dimensions, the vector potential is defined in relation to the velocity vector field,

$$\vec{u} = \vec{u}(x,y,z;t) = \nabla \times \vec{\psi} \tag{6.2}$$

where $\vec{\psi} = \vec{\psi}(x,y,z;t)$. This is shown in figure 6.1a. Once again, similarly to the streamfunction, the vector potential is a mathematical idealisation which arises and exists

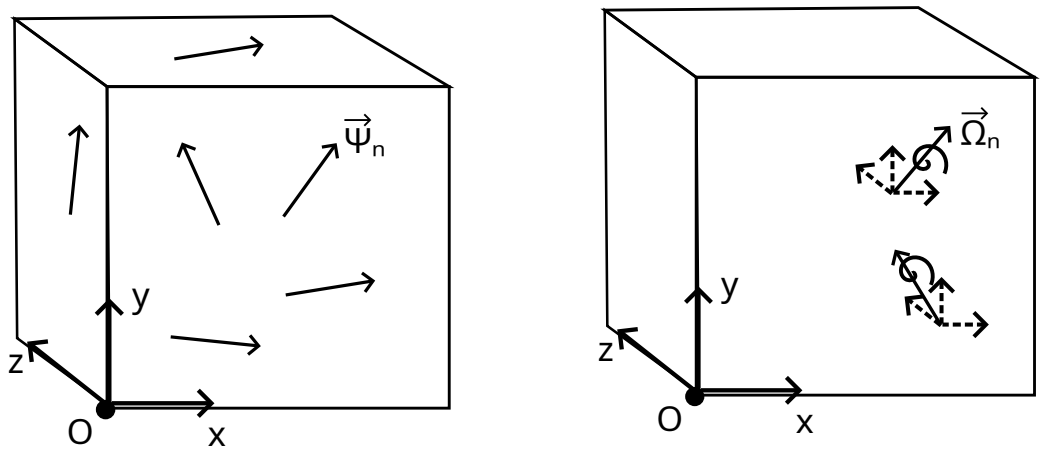

(a) Vector potential, $\vec{\psi}(x,y,z;t)$ (b) Vorticity, $\vec{\Omega}(x,y,z;t)$

Figure 6.1: Conceptual drawing of $\vec{\psi}$ and $\vec{\Omega}$ in three dimensions

only in the light of our assumption of constant density. As we did with the streamfunction, we can use it to describe the three dimensional velocity field. It is responsible for upholding the divergence-free velocity constraint.

We substitute our equation 6.2 into the divergence-free velocity constraint,

$$\nabla \cdot \vec{u} = \nabla \cdot (\nabla \times \vec{\psi}) = 0 \tag{6.3}$$

This is identically zero, and hence the vector potential automatically satisfies incompressible continuity in the physics. Numerically, this will not be satisfied and we use the divergence of velocity and divergence of vorticity as markers of success of our numerical solution. In practice the divergence of velocity constraint is quite easy to satisfy as least for low *Re* in the cases studied. This is not true of the divergence of vorticity constraint.

We now consider an identity with an arbitrary vector $\vec{a}$,

$$\nabla^2 \vec{a} = \nabla(\nabla \cdot \vec{a}) - \nabla \times (\nabla \times \vec{a}) \tag{6.4}$$

Let $\vec{a} = \vec{\psi}$,

$$\nabla^2 \vec{\psi} = \nabla(\nabla \cdot \vec{\psi}) - \nabla \times (\nabla \times \vec{\psi}) \tag{6.5}$$

Substitute equation 6.2 and consider that the first term on the right hand side disappears, then

$$\boxed{\nabla^2 \vec{\psi} = -\vec{\Omega}} \tag{6.6}$$

Here we have the ***vector potential Poisson equation*** Thus we have one relationship between the vector potential and the vorticity to draw upon.

Writing equation 6.6 in scalar form gives,

$$\nabla^2 \psi_x \vec{e}_x + \nabla^2 \psi_y \vec{e}_y + \nabla^2 \psi_z \vec{e}_z = -(\Omega_x \vec{e}_x + \Omega_y \vec{e}_y + \Omega_z \vec{e}_z) \tag{6.7}$$

Which can be separated into each of the x, y, and z components. Thus we have the first step of our algorithm. The second relationship we use relates the velocity vector field to the vector potential field as shown in equation 6.2 and it is repeated here. The ***vector potential equation***,

$$\boxed{\vec{u} = \nabla \times \vec{\psi}} \tag{6.8}$$

Finally we have the full ***three dimensional vorticity transport equation*** which includes the stretching term as shown in equation 4.40 and repeated here,

$$\boxed{\frac{\partial \vec{\Omega}}{\partial t} + (\vec{u} \cdot \nabla)\vec{\Omega} - (\vec{\Omega} \cdot \nabla)\vec{u} = \nu \nabla^2 \vec{\Omega}} \tag{6.9}$$

This too can be written in scalar form for discretisation. Thus, these three relationships are used in our algorithm as outlined below.

6.2 The Algorithm

I . **Solve three Poisson equations for the vector potential field:**

$$\nabla^2 \psi_x = \frac{\partial^2 \psi_x}{\partial x^2} + \frac{\partial^2 \psi_x}{\partial y^2} + \frac{\partial^2 \psi_x}{\partial z^2} = -\Omega_x = -\left(\frac{\partial w}{\partial y} - \frac{\partial v}{\partial z}\right) \tag{6.10}$$

$$\nabla^2 \psi_y = \frac{\partial^2 \psi_y}{\partial x^2} + \frac{\partial^2 \psi_y}{\partial y^2} + \frac{\partial^2 \psi_y}{\partial z^2} = -\Omega_y = -\left(\frac{\partial u}{\partial z} - \frac{\partial w}{\partial x}\right) \tag{6.11}$$

$$\nabla^2 \psi_z = \frac{\partial^2 \psi_z}{\partial x^2} + \frac{\partial^2 \psi_z}{\partial y^2} + \frac{\partial^2 \psi_z}{\partial z^2} = -\Omega_z = -\left(\frac{\partial v}{\partial x} - \frac{\partial u}{\partial y}\right) \tag{6.12}$$

II . **Compute the velocity vector field:**

$$\vec{u} = u\vec{e}_x + v\vec{e}_y + w\vec{e}_z = \nabla \times \vec{\psi} \tag{6.13}$$

Which using the cross product yields,

$$u = \frac{\partial \psi_z}{\partial y} - \frac{\partial \psi_y}{\partial z} \tag{6.14}$$

$$v = \frac{\partial \psi_x}{\partial z} - \frac{\partial \psi_z}{\partial x} \tag{6.15}$$

$$w = \frac{\partial \psi_y}{\partial x} - \frac{\partial \psi_x}{\partial y} \tag{6.16}$$

III . **Solve the three dimensional vorticity transport equation which includes the vortex stretching term:**

$$\frac{\partial \vec{\Omega}}{\partial t} + (\vec{u} \cdot \nabla)\vec{\Omega} - (\vec{\Omega} \cdot \nabla)\vec{u} = \nu \nabla^2 \vec{\Omega} \tag{6.17}$$

Crucially, this includes the vortex stretching term. Writing this in scalar form so that there are three equations, one for each Cartesian coordinate,

$$\frac{\partial \Omega_x}{\partial t} + u\frac{\partial \Omega_x}{\partial x} + v\frac{\partial \Omega_x}{\partial y} + w\frac{\partial \Omega_x}{\partial z} - \Omega_x\frac{\partial u}{\partial x} - \Omega_y\frac{\partial u}{\partial y} - \Omega_z\frac{\partial u}{\partial z} = \nu\left(\frac{\partial^2 \Omega_x}{\partial x^2} + \frac{\partial^2 \Omega_x}{\partial y^2} + \frac{\partial^2 \Omega_x}{\partial z^2}\right) \tag{6.18}$$

$$\frac{\partial \Omega_y}{\partial t} + u\frac{\partial \Omega_y}{\partial x} + v\frac{\partial \Omega_y}{\partial y} + w\frac{\partial \Omega_y}{\partial z} - \Omega_x\frac{\partial v}{\partial x} - \Omega_y\frac{\partial v}{\partial y} - \Omega_z\frac{\partial v}{\partial z} = \nu\left(\frac{\partial^2 \Omega_y}{\partial x^2} + \frac{\partial^2 \Omega_y}{\partial y^2} + \frac{\partial^2 \Omega_y}{\partial z^2}\right) \tag{6.19}$$

$$\frac{\partial \Omega_z}{\partial t} + u\frac{\partial \Omega_z}{\partial x} + v\frac{\partial \Omega_z}{\partial y} + w\frac{\partial \Omega_z}{\partial z} - \Omega_x\frac{\partial w}{\partial x} - \Omega_y\frac{\partial w}{\partial y} - \Omega_z\frac{\partial w}{\partial z} = \nu\left(\frac{\partial^2 \Omega_z}{\partial x^2} + \frac{\partial^2 \Omega_z}{\partial y^2} + \frac{\partial^2 \Omega_z}{\partial z^2}\right) \tag{6.20}$$

6.3 Boundary Conditions

6.3.1 $\vec{\psi}$ Boundary Conditions

Boundary conditions were derived according to Tokunaga [13]. Define the $\vec{\psi}$ vector in the normal and tangential directions as $\vec{\psi}_n$, $\vec{\psi}_{\tau_1}$, $\vec{\psi}_{\tau_2}$, where n, τ_1, and τ_2 are the unit vectors, then according to Tokunaga we have,

$$\frac{\partial \vec{\psi}_n}{\partial n} = \vec{\psi}_{\tau_1} = \vec{\psi}_{\tau_2} = 0 \tag{6.21}$$

This implies that the tangential components of $\vec{\psi}$ on the wall vanish. We use a Taylor series expansion of the remaining normal derivative of the normal component to acquire a value for $\vec{\psi}$ on the wall. The Taylor expansion is for the value of $\vec{\psi}$ one step away from the wall using the value of $\vec{\psi}$ and its derivatives at the wall, rearranged for the first derivative.

As an example, we show the left wall,

$$\psi_{1,j,k} = \psi_{0,j,k} + \left.\frac{\partial \psi}{\partial x}\right|_{0,j,k}\Delta x + \frac{1}{2!}\left.\frac{\partial^2 \psi}{\partial x^2}\right|_{0,j,k}(\Delta x)^2 + \frac{1}{3!}\left.\frac{\partial^3 \psi}{\partial x^3}\right|_{0,j,k}(\Delta x)^3 + \ldots \tag{6.22}$$

Rearranging for the first derivative, and neglecting higher order terms, we will have an error which scales with Δx. Combine this with equation 6.21,

$$\left.\frac{\partial \psi}{\partial x}\right|_{0,j,k} = \frac{\psi_{1,j,k} - \psi_{0,j,k}}{\Delta x} + O(\Delta x) = 0 \tag{6.23}$$

Implying,

$$\psi_{x,0,j,k} = \psi_{x,1,j,k} \tag{6.24}$$

$$\psi_y = 0.0 \tag{6.25}$$

$$\psi_z = 0.0 \tag{6.26}$$

A similar process is used for the rest of the walls, including the top wall. Essentially, the tangential components of ψ disappear, and the normal component takes the value from one step inside the domain.

6.3.2 $\vec{u}$ Boundary Conditions

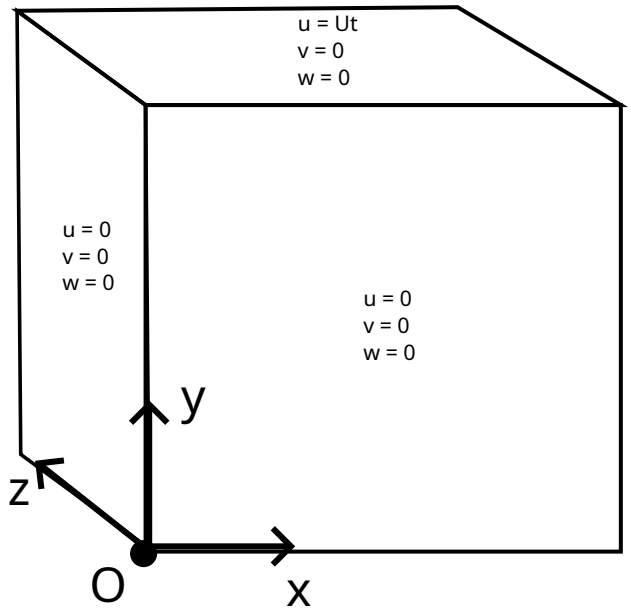

Figure 6.2: Velocity boundary conditions for a three dimensional cubic cavity

Consider that $\vec{u} = u\vec{e}_x + v\vec{e}_y + w\vec{e}_z$. Velocity boundary conditons are imposed simply as in figure 6.2. Thus, in this algorithm the top wall velocity is not entering the physics by the $\vec{\psi}$ boundary conditions but through application of the $\vec{u}$ boundary conditions on each step as well as the top wall vorticity boundary condition.

6.3.3 $\vec{\Omega}$ Boundary Conditions

To demonstrate the method, boundary conditions for vorticity on the left wall are derived.

We have,

$$\vec{\Omega} = \nabla \times \vec{u} \tag{6.27}$$

Which when expanded becomes,

$$\vec{\Omega} = \Omega_x\vec{e}_x + \Omega_y\vec{e}_y + \Omega_z\vec{e}_z = \left(\frac{\partial w}{\partial y} - \frac{\partial v}{\partial z}\right)\vec{e}_x + \left(\frac{\partial u}{\partial z} - \frac{\partial w}{\partial x}\right)\vec{e}_y + \left(\frac{\partial v}{\partial x} - \frac{\partial u}{\partial y}\right)\vec{e}_z \tag{6.28}$$

Considering the left wall of the cubic cavity, we approximate the first derivatives of the velocity components on the wall by using a finite difference based on a Taylor series expansion. The value of the first derivatives of the velocity components on the wall are approximated using the derivatives one step out from the wall.

Consider the x component of vorticity directly on the left wall,

$$\Omega_x|_{0,j,k} = \left.\frac{\partial w}{\partial y}\right|_{0,j,k} - \left.\frac{\partial v}{\partial z}\right|_{0,j,k} \tag{6.29}$$

For the first velocity derivative in equation 6.29, use a Taylor series expansion,

$$w_{0,j+1,k} = w_{0,j,k} + \left.\frac{\partial w}{\partial y}\right|_{0,j,k} \Delta y + \frac{1}{2!}\left.\frac{\partial^2 w}{\partial y^2}\right|_{0,j,k} (\Delta y)^2 + \frac{1}{3!}\left.\frac{\partial^3 w}{\partial y^3}\right|_{0,j,k} (\Delta y)^3 + \ldots \tag{6.30}$$

Rearranging for the first derivative as required,

$$\left.\frac{\partial w}{\partial y}\right|_{0,j,k} = \frac{w_{0,j+1,k} - w_{0,j,k}}{\Delta y} - \frac{1}{2!}\left.\frac{\partial^2 w}{\partial y^2}\right|_{0,j,k} \Delta y - \frac{1}{3!}\left.\frac{\partial^3 w}{\partial y^3}\right|_{0,j,k} (\Delta y)^2 - \ldots \tag{6.31}$$

Neglecting higher order terms,

$$\left.\frac{\partial w}{\partial y}\right|_{0,j,k} = \frac{w_{0,j+1,k} - w_{0,j,k}}{\Delta y} + O(\Delta y) \tag{6.32}$$

This is a *first-order* or *first-order accurate* finite difference for the first derivative of the velocity component. This name is given because the leading error term which is neglected scales with a grid size of the order Δx. It is a *forward* difference, as it uses a value one point ahead to update the current value.

For the second velocity derivative in equation 6.29,

$$v_{0,j,k+1} = v_{0,j,k} + \left.\frac{\partial v}{\partial z}\right|_{0,j,k} \Delta z + \frac{1}{2!}\left.\frac{\partial^2 v}{\partial z^2}\right|_{0,j,k} (\Delta z)^2 + \frac{1}{3!}\left.\frac{\partial^3 v}{\partial z^3}\right|_{0,j,k} (\Delta z)^3 + \ldots \tag{6.33}$$

Therefore, rearranging for the first derivative as required,

$$\left.\frac{\partial v}{\partial z}\right|_{0,j,k} = \frac{v_{0,j,k+1} - v_{0,j,k}}{\Delta z} - \frac{1}{2!}\left.\frac{\partial^2 v}{\partial z^2}\right|_{0,j,k} \Delta z - \frac{1}{3!}\left.\frac{\partial^3 v}{\partial z^3}\right|_{0,j,k} (\Delta z)^2 - \ldots \tag{6.34}$$

Neglecting higher order terms,

$$\left.\frac{\partial v}{\partial z}\right|_{0,j,k} = \frac{v_{0,j,k+1} - v_{0,j,k}}{\Delta z} + O(\Delta z) \tag{6.35}$$

Repeating this process for the other vorticity components, we have

$$\Omega_x = \frac{w_{0,j+1,k} - w_{0,j,k}}{\Delta y} - \left(\frac{v_{0,j,k+1} - v_{0,j,k}}{\Delta z}\right) \tag{6.36}$$

$$\Omega_y = \frac{u_{0,j,k+1} - u_{0,j,k}}{\Delta z} - \left(\frac{w_{1,j,k} - w_{0,j,k}}{\Delta x}\right) \tag{6.37}$$

$$\Omega_z = \frac{v_{1,j,k} - v_{0,j,k}}{\Delta x} - \left(\frac{u_{0,j+1,k} - w_{0,j,k}}{\Delta y}\right) \tag{6.38}$$

on the left wall.

Considering figure 6.2, all velocity components at points directly on the wall are zero. Therefore, equations 6.36 - 6.38, become $\Omega_x = 0$, $\Omega_y = -w_{1,j,k}/\Delta x$, $\Omega_z = v_{1,j,k}/\Delta x$. Clearly, we see that only vorticity components involving a derivative normal to the wall in question are non-zero; and the vorticity on the wall becomes equal to the value of a velocity component one step off of the wall.

6.4 Link to the Code

The following is a link to the public GitHub repository housing the code corresponding to this section. The $\vec{\psi} - \vec{\Omega}$ formulation code can be found under the directory name '*vector_psi_omega*'. Please read the '*README.md*' file for further details about the repository:

`https://github.com/abrierley0/incompressible_repo/tree/main`

Chapter 7

The Three-dimensional Lid-Driven Cube

As commented by Weinan and Liu [9], the divergence of velocity is satisfied in the physics automatically. This can explain our only small error in figures 7.11 and 7.12 for the divergence of the velocity on the centreplane and outer plane respectively. Likely, these small errors in divergence of velocity arise only from rounding errors of the machine. They are only of order 10^{-15} and are small even on the outer plane. They do increase mildly with *Re* but remain negligible. There does not seem to be much difference between central and outer plane as shown in figures 7.11 and 7.12 for the divergence of velocity. However, we may see divergence of velocity increase for higher *Re*. Divergence of vorticity, on the other hand, is high near the discontinuities at the upper corners. This is consistent across all *Re* and increases with *Re*. Divergence of vorticity is worse on the outer planes compared to that on the central planes, across *Re*. This is a problem, and consistent with Weinan and Liu, who suggest the primary difficulty for this formulation is in enforcing divergence free vorticity at the corner points.

It is perhaps hoped that the divergence of vorticity remains contained in the corners and does not propagate into the cavity. Even in the corners, it is not optimal, especially if we would like to investigate flows in three dimensional corners. But, as suggested by Weinan and Liu, the divergence on the boundary can often dictate divergence within the cavity. This is somewhat evident from figure 7.13; divergence of vorticity has entered the centre of the primary eddy. Notedly, there is less of this for *Re* = 1000, however the vorticity divergence does propagate down into the cavity at the downstream wall (figure 7.18). For the centre plane, at low Reynolds' number, the divergence of vorticity is of the order 1. This might be acceptable, especially considering the agreement on velocity centrelines. Good agreement for velocity centrelines in a 3D cube with the paper by Chen

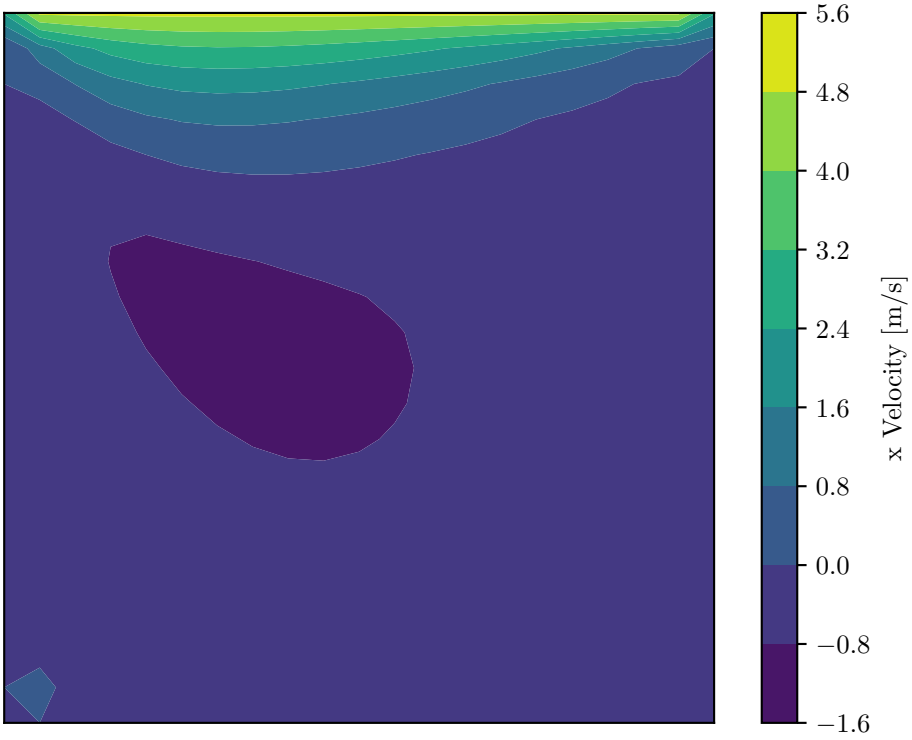

Figure 7.1: x velocity on (x, y, 0.5) at Re = 100

et al. for Re = 100 is found in this case, as shown in figure 7.5. Though there is some discrepancy in the centre of the eddy, this is likely a case of optimising simulation parameters; the same can be said for higher *Re*. The centre of the eddy has vorticity divergence approaching 1 suggesting the error may be propagating into the cavity. This is contrary to the $\psi - \Omega$ case, where there was high vorticity divergence in the corners, but it did not seem to propagate into the centre of the cavity (see figure 5.15). The reason for propagation in the three dimensional case may be due to cross-flows, for example considering figure 7.3, where there is some velocity in the spanwise direction. The discrepancy in velocity profiles for higher *Re* as shown in figure 7.5 is not a matter of correctness but of running the simulation for more physical time or shorter time steps or with different Poisson parameters. Discrepancy increasing for *Re* = 400 then *Re* = 1000 is probably to be down to a coarse grid or simply suboptimal simulation parameters rather than error with the solver itself.

	100	400	1000
Run	11	16	17
nx	21	64	64
dt (s)	$2.0e^{-3}$	$4.75e^{-5}$	$4.75e^{-5}$
Ω_{conv}	0.1	0.1	0.1
β	1.0	1.0	1.0
tol	0.0001	0.0001	0.0001
itmax	1000	1000	1000
t_{end} (mins)	1.0	1.23	0.86
t_{wall} (hrs)	0.35	1.65	6.92
Iterations	495	2584	18070

Table 7.1: Table showing the simulation parameters used to generate the results

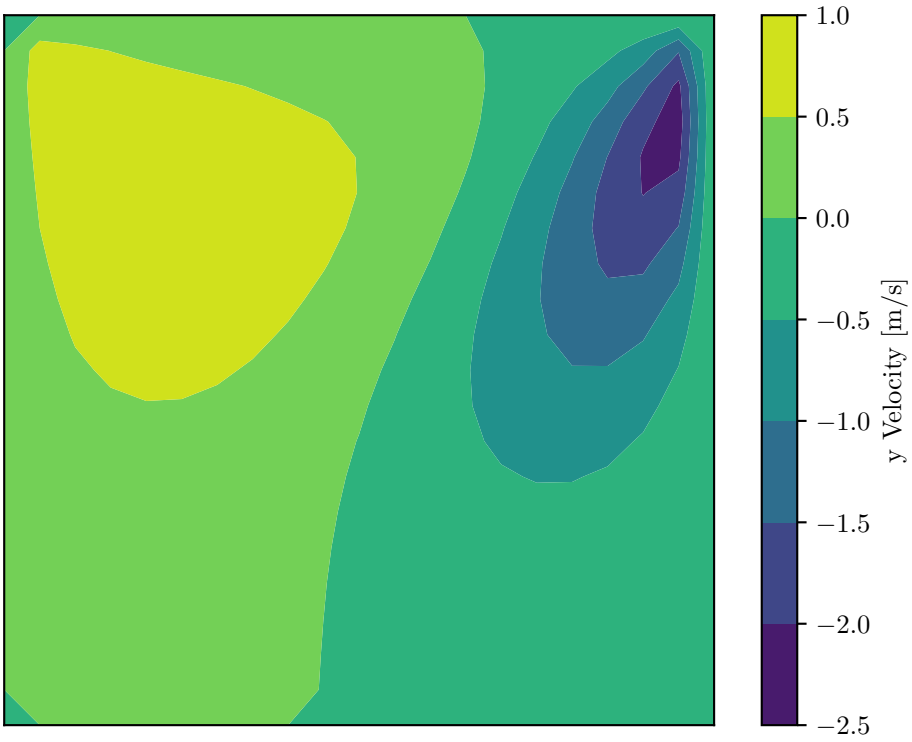

Figure 7.2: y velocity on (x, y, 0.5) at Re = 100

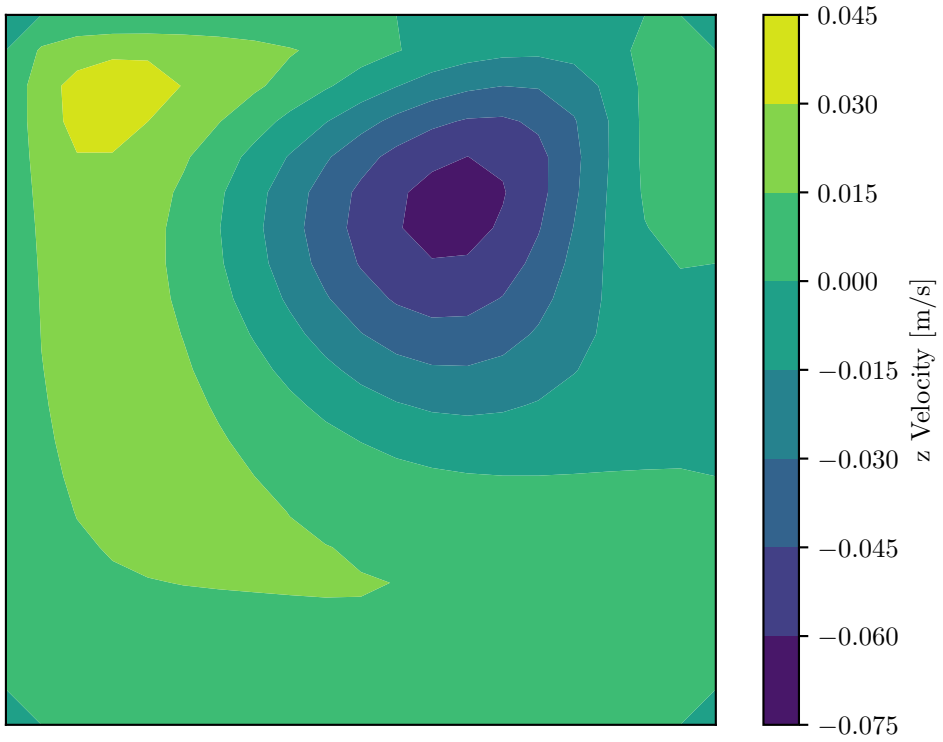

Figure 7.3: z velocity on (x, y, 0.5) at Re = 100

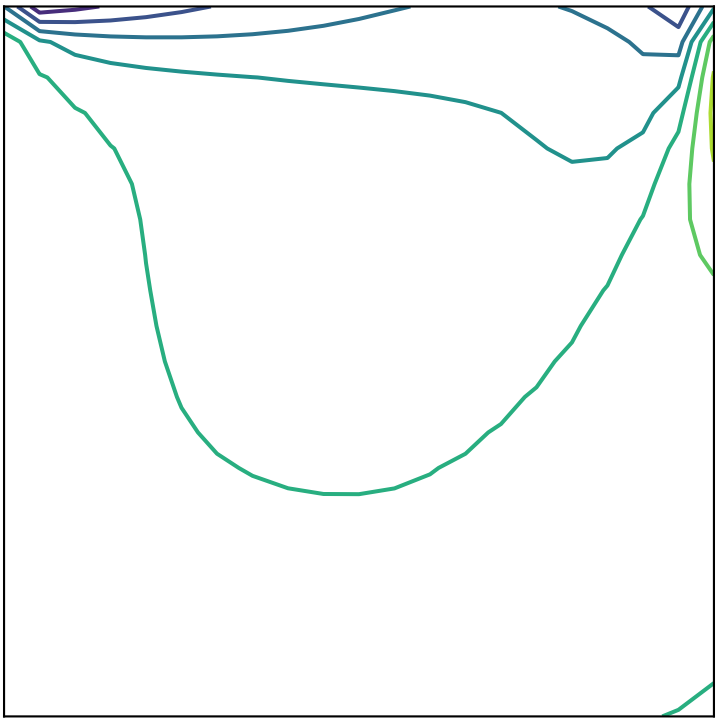

Figure 7.4: z vorticity on (x, y, 0.5) at Re = 100

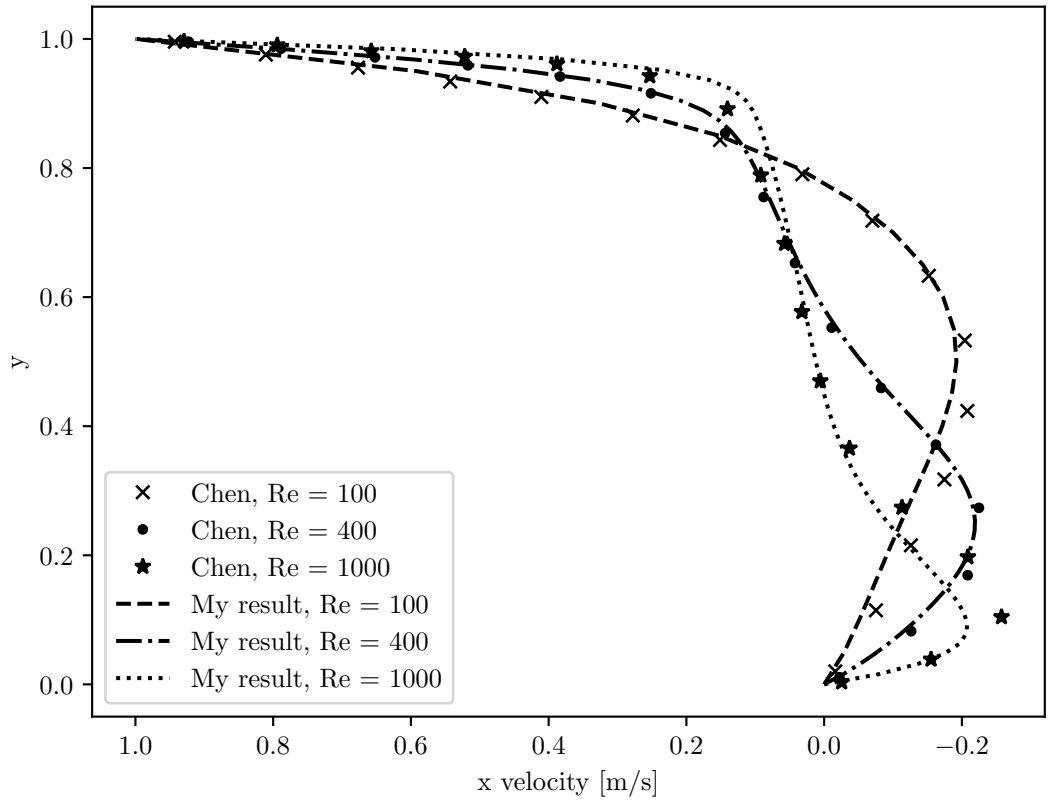

Figure 7.5: x Velocity centrelines on (x, y, 0.5)

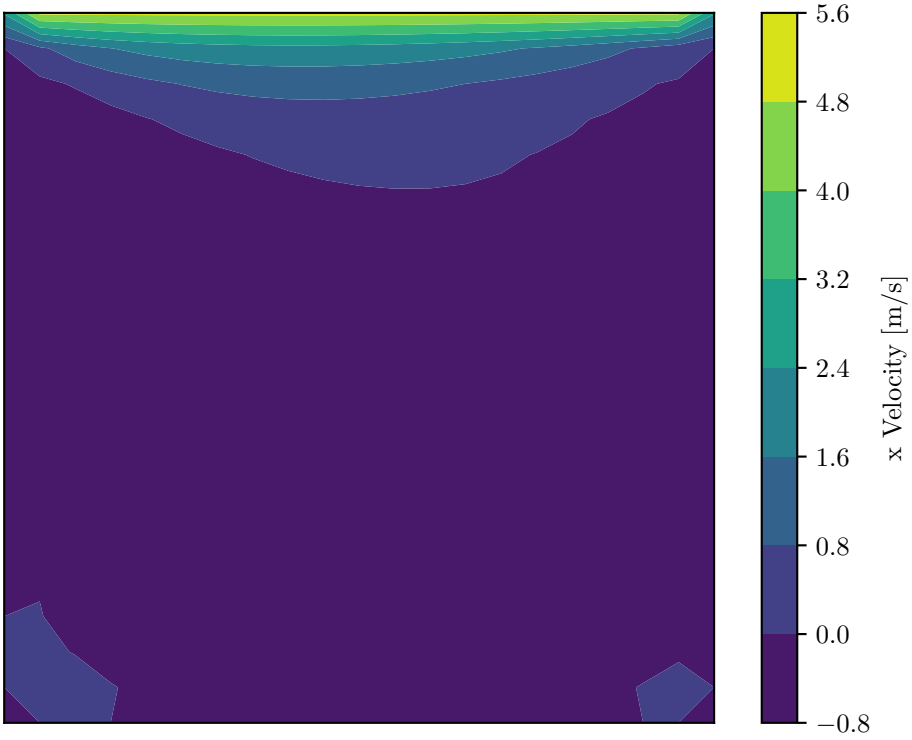

Figure 7.6: x velocity on (x, y, 0.95) at Re = 100

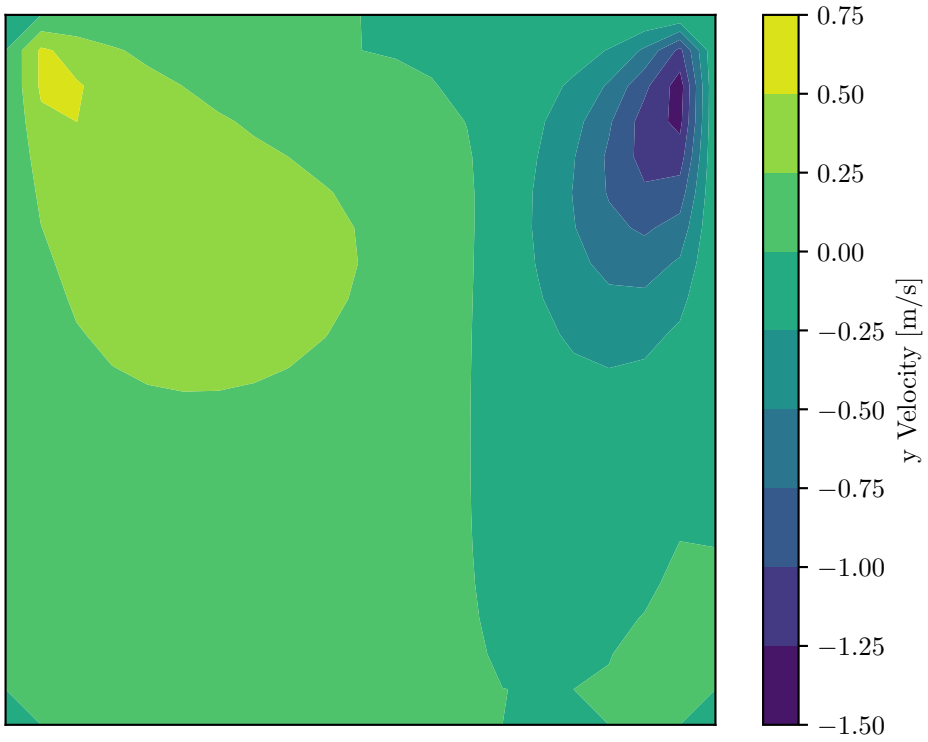

Figure 7.7: y velocity on (x, y, 0.95) at Re = 100

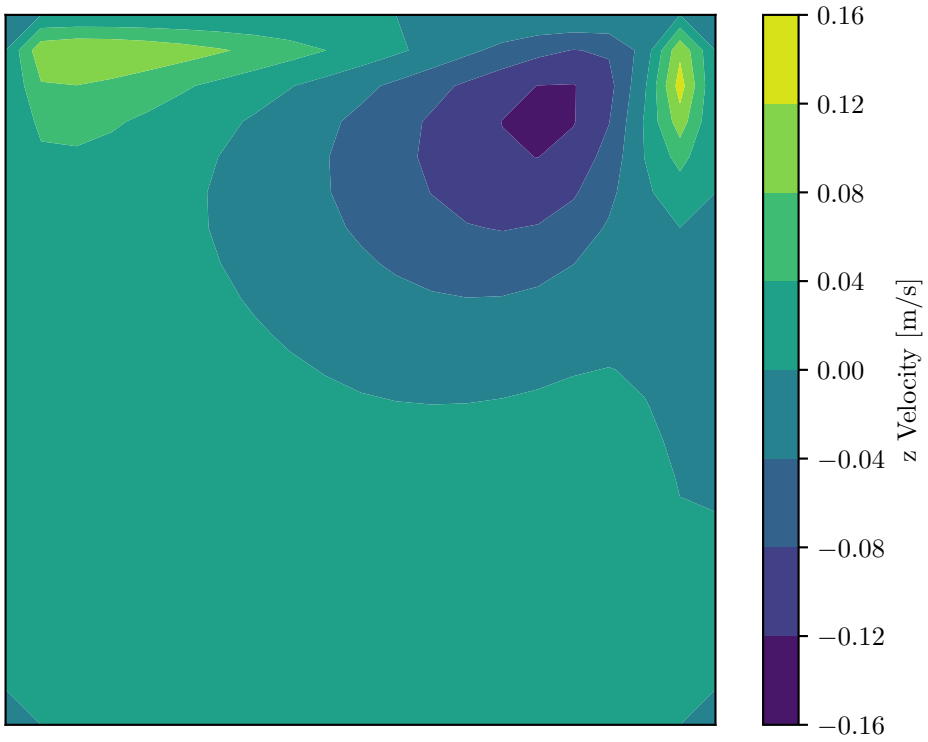

Figure 7.8: z velocity on (x, y, 0.95) at Re = 100

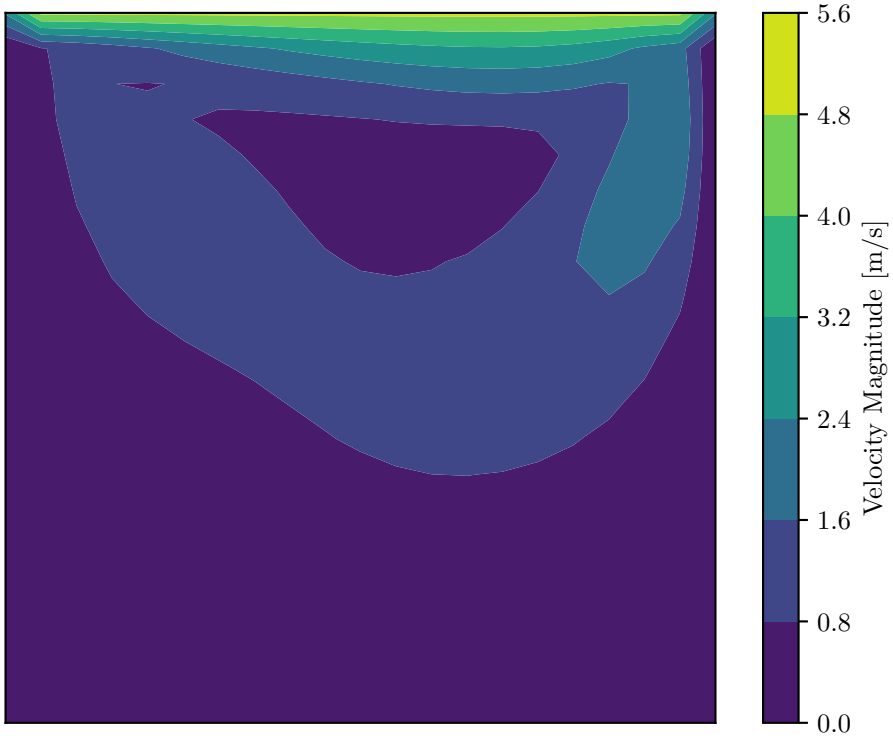

Figure 7.9: Velocity magnitude on (x, y, 0.5) at Re = 100

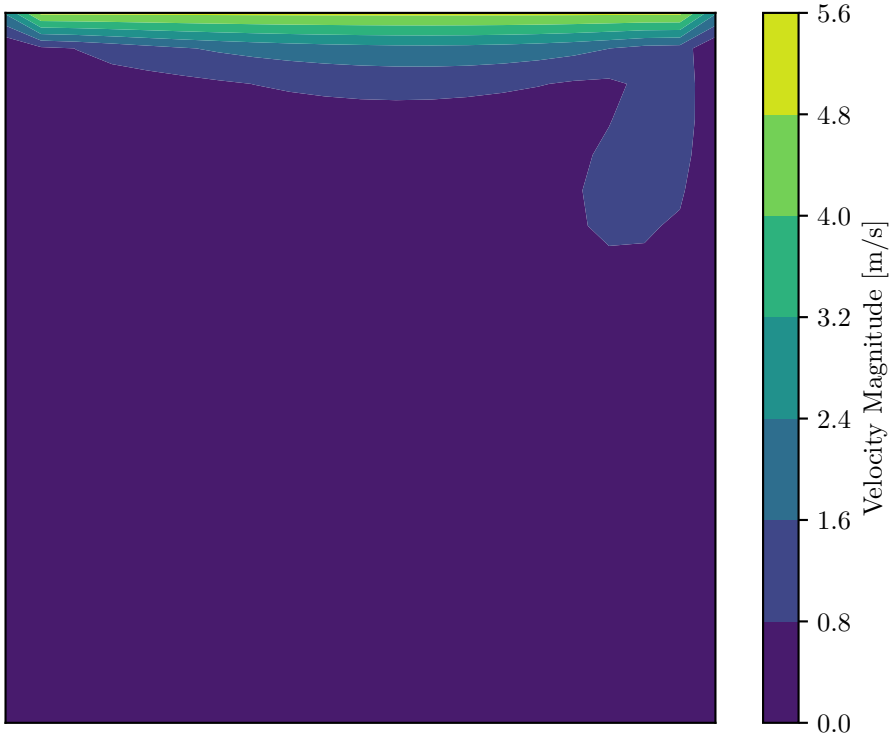

Figure 7.10: Velocity magnitude on (x, y, 0.95) at Re = 100

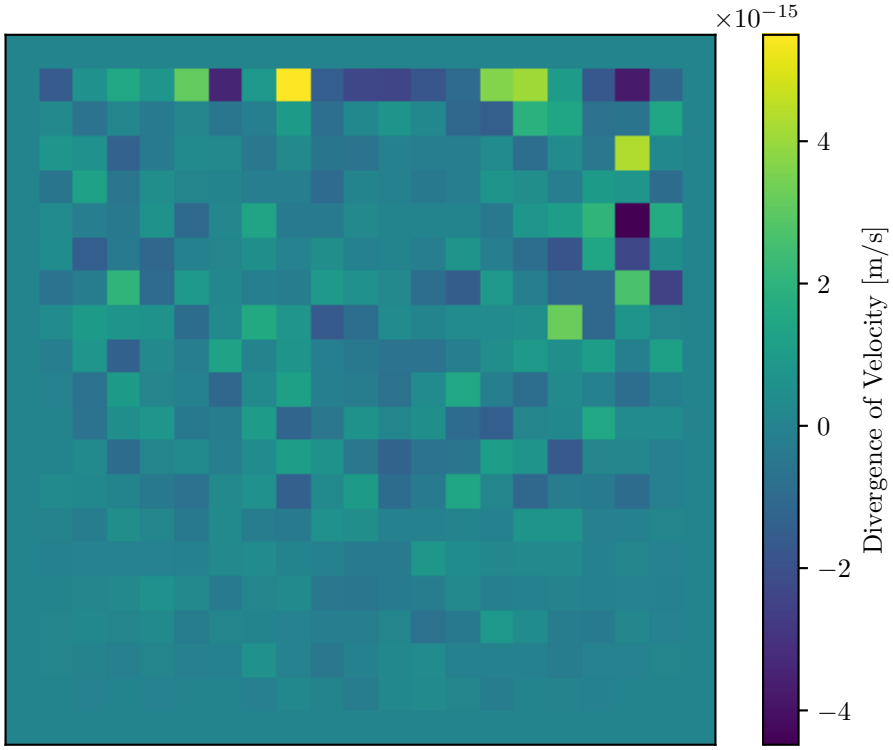

Figure 7.11: Divergence of velocity on (x, y, 0.5) at Re = 100

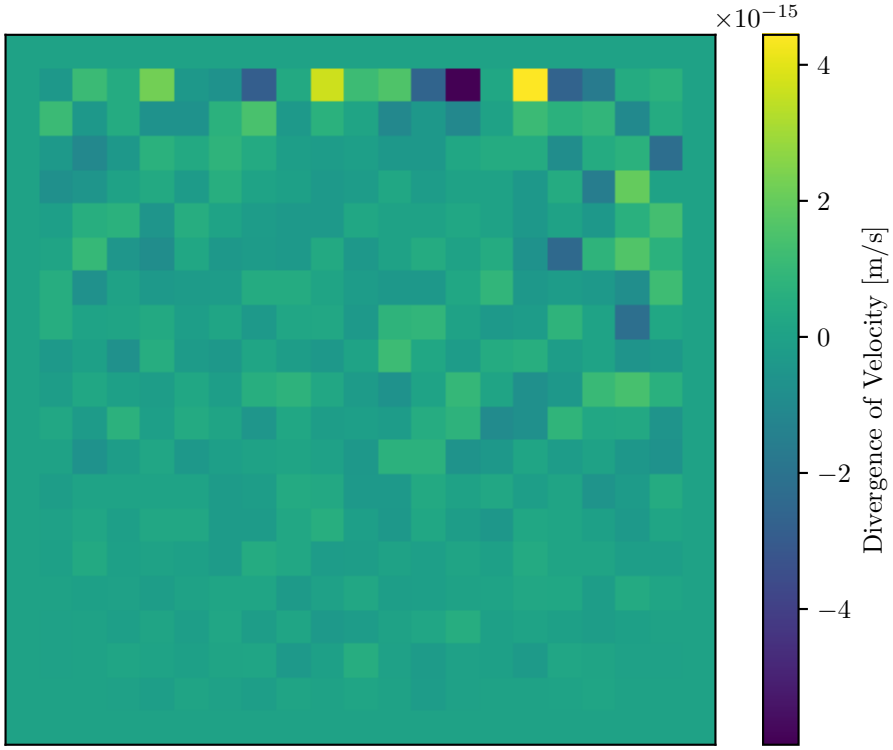

Figure 7.12: Divergence of velocity on (x, y, 0.95) at Re = 100

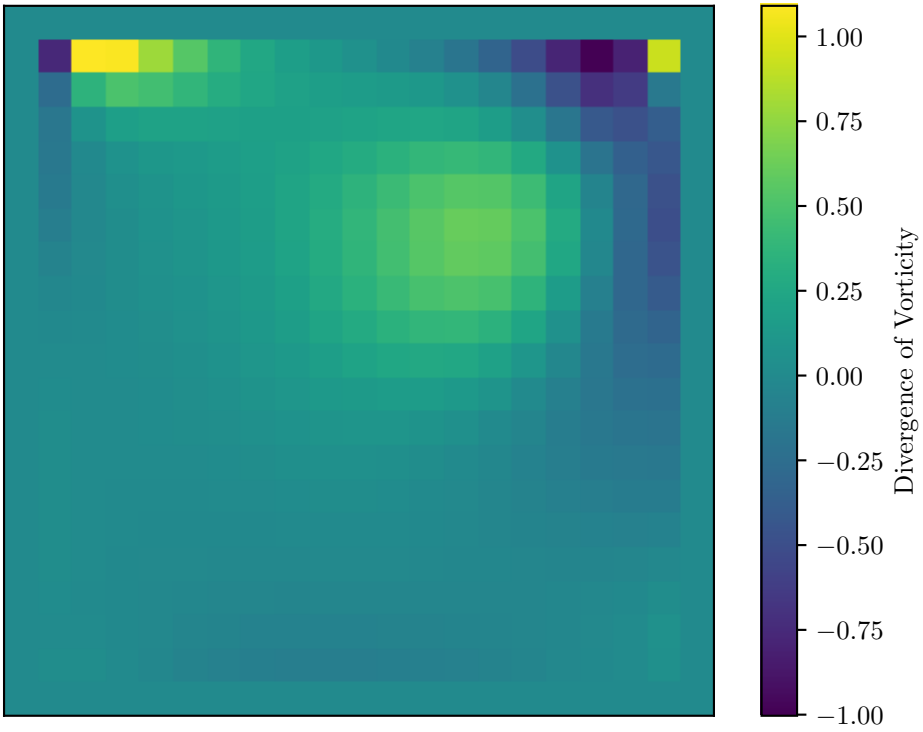

Figure 7.13: Divergence of vorticity on (x, y, 0.5) at Re = 100

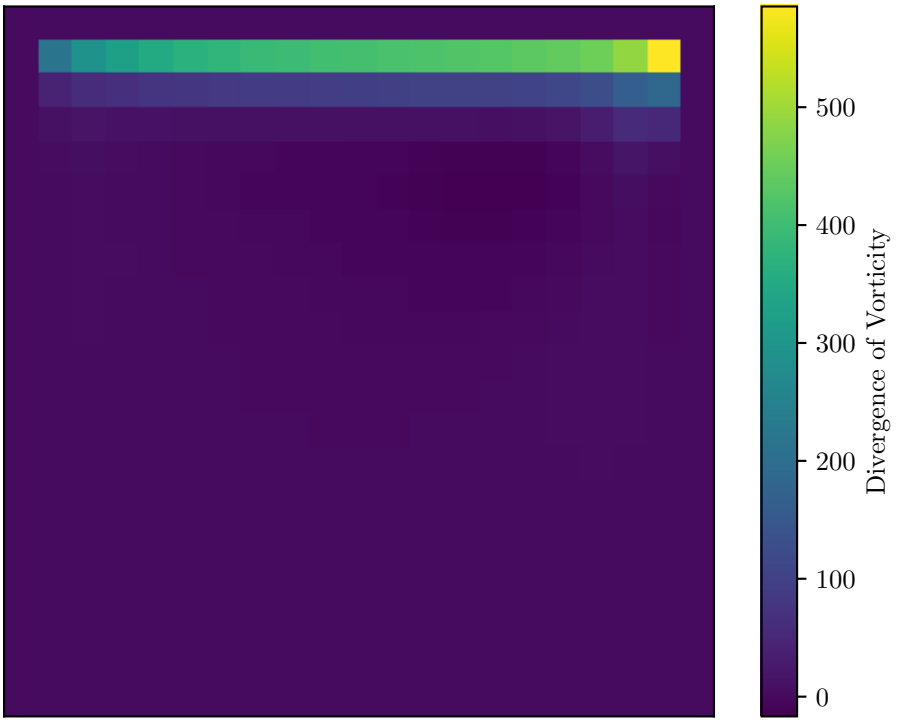

Figure 7.14: Divergence of vorticity on (x, y, 0.95) at Re = 100

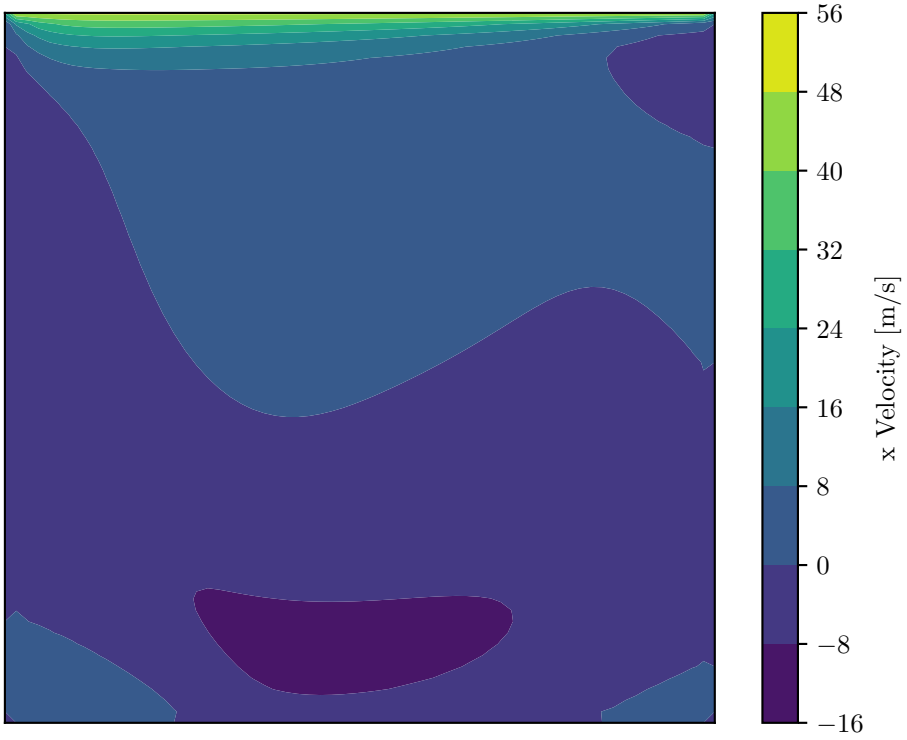

Figure 7.15: x Velocity on (x, y, 0.5) at Re = 1000

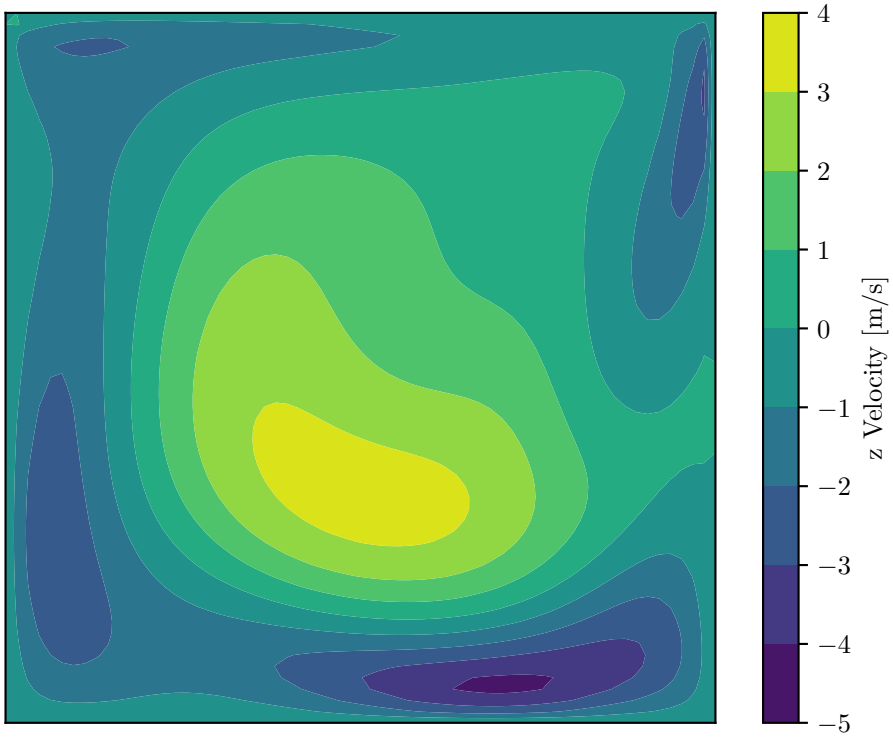

Figure 7.16: z Velocity on (x, y, 0.5) at Re = 1000

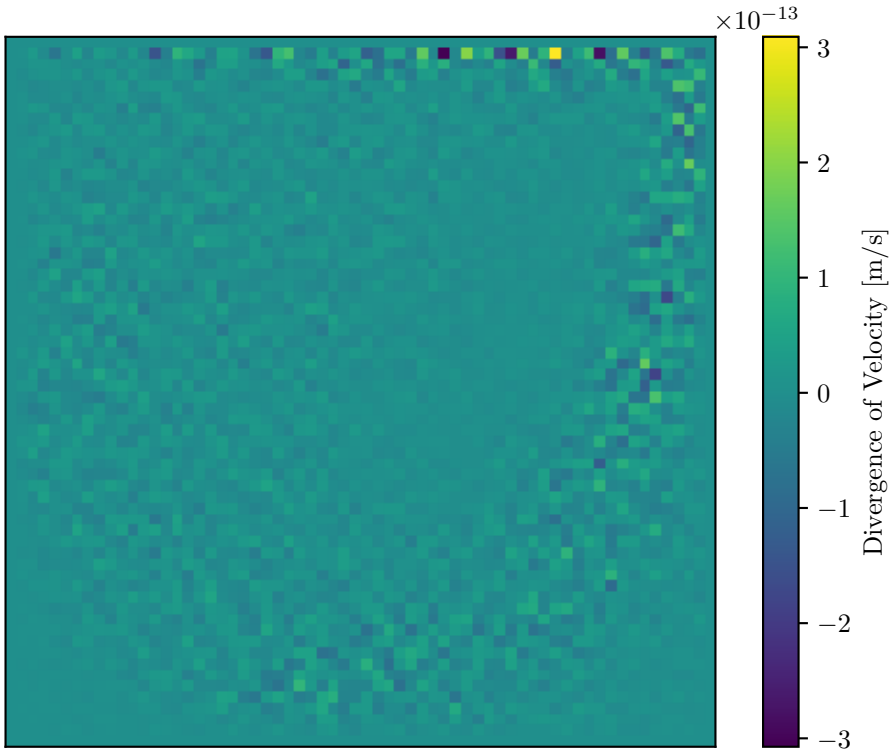

Figure 7.17: Divergence of velocity on (x, y, 0.5) at Re = 1000

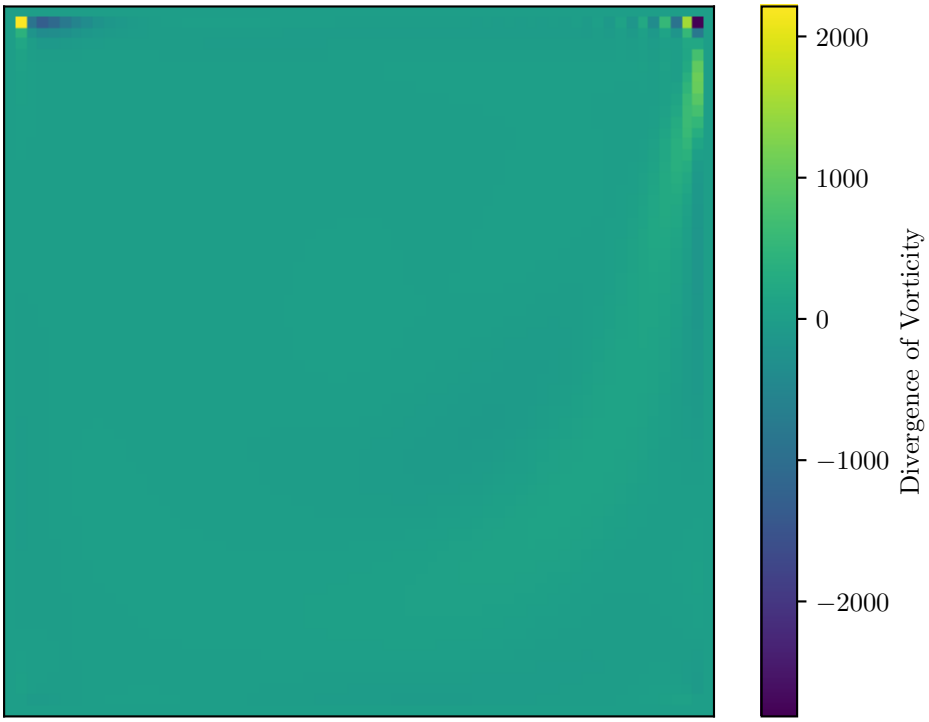

Figure 7.18: Divergence of vorticity on (x, y, 0.5) at Re = 1000

Chapter 8

Future Work

The thesis has produced a working $\psi - \Omega$ code, and importantly a working $\vec{\psi} - \vec{\Omega}$ code. The results have been validated against the literature and it can be seen that the implementation and formulation are at least correct, and problems with accuracy only require optimised simulation parameters. This is true for the *Re* range covered, but not may not be the case for *Re* higher than 1000.

Furthermore, a grid convergence study was not carried out. This should be done. It may explain discrepancies for the velocity on the centrelines in the $\vec{\psi} - \vec{\Omega}$ method. Validation should also be completed for other benchmarks, such as duct or channel flow, which may reveal issues with the solvers not evident in the cubic cavity test case.

In future the focus would be to try to reduce or eliminate divergence of vorticity. Alternative discretisation of the non-linear convective term seems promising. Furthermore, work on the vorticity boundary condtions has potential, and it may be possible to select a palette of higher order schemes which will satisfy the divergence constraints algebraically, perhaps with the help of symbolic maths software, or even AI.

The effect of the high divergence of vorticity near the corners, which has sometimes propagated into the internal domain, on the overall accuracy of the solver has not been analysed. Conceivably, judging by the velocity centreline plots, the flow is correct. However, velocity centrelines closer to the wall have not been plotted. We would expect the accuracy to be suboptimal the closer we get to the wall. Most of the future work would be ensuring accurate flow in the near wall region.

Efforts could also be made to speed up the solver, for example with multiple processors, GPU, or C-based optimisation. Studies into the stability of these cases could be

conducted, which do not currently exist for three dimensions.

Fixing the divergence of vorticity constraint will enable the working code to be extended to more complex geometries, like curvilinear domains, higher Re, and cases such as transition and turbulence where potentially new physics could be discovered. The existence in the physics of the vortex stretching term makes this an interesting prospect.

Chapter 9

Appendix

9.1 CURES Approval Letter

6 June 2025

Dear Mr Brierley ,

Reference: CURES/25560/2025
Project ID: 29130
Title: Implementation of the Vector-Potential and Vorticity Transport Formulation for Simulating Newtonian Fluid Flows in a Three-Dimensional Rectangular Channel

We are pleased to inform you that you have successfully declared that your research project is a **Literature Review – based solely on openly available literature which is in the public domain, and you are undertaking desk-based research not involving any other form of data or information.**

You have also confirmed that your project **does not meet** any of the literature review specified exceptions, listed both within the relevant section of the CURES form and below:

1) Your supervisor has requested that you apply for approval through CURES because:

- The journals or data are in a sensitive area (please discuss this with your supervisor)
- The project will be embargoed **i.e. will not be publicly available via the Cranfield library immediately or longer term**

2) Approval is/will be specifically required by another external body e.g. journal publishers

Therefore, **you do not require ethical approval** and your CURES application will be automatically closed.

Please keep a copy of this letter safe, if this exception is in relation to your thesis project, you will need to include a copy with your final thesis submission.

If you have any queries, please contact CURES Support.

We wish you every success with your project.

Regards,

CURES Team

Bibliography

[1] Kawaguti M. Numerical Solution of the Navier-Stokes Equations for the Flow in a Two-Dimensional Cavity. Journal of the Physical Society of Japan. 1961 Nov;16(11):2307-15.

[2] Burggraf OR. Analytical and numerical studies of the structure of steady separated flows. Journal of Fluid Mechanics. 1966 Jan;24(1):113-51.

[3] Helmholtz H. Ãber Integrale der hydrodynamischen Gleichungen, welche den Wirbelbewegungen entsprechen. Journal fÃŒr die reine und angewandte Mathematik. 1858.

[4] Lamb H. Hydrodynamics. 6th ed. Cambridge University Press; 1879.

[5] Prandtl L. Uber Flussigkeitsbewegung bei sehr kleiner Reibung. 1904.

[6] Thom A. The Flow Past Circular Cylinders at Low Speeds. Proceedings of the Royal Society of London A. 1933;141(843):651-69.

[7] Batchelor GK. On steady laminar flow with closed streamlines at large Reynolds number. Journal of Fluid Mechanics. 1956 Jul;1(2):177-90.

[8] Kuhlmann HC, Romanó F. In: The Lid-Driven Cavity. Springer International Publishing; 2018. p. 233-309.

[9] E W, Liu JG. Finite Difference Methods for 3D Viscous Incompressible Flows in the VorticityâVector Potential Formulation on Nonstaggered Grids. Journal of Computational Physics. 1997 Nov;138(1):57-82.

[10] Taylor GI. On Scraping Viscous Fluid From a Plane Surface. Volume IV: Mechanics of Fluids: Miscellaneous Papers. 1971;4:410-3.

[11] Moffatt HK. Viscous and resistive eddies near a sharp corner. Journal of Fluid Mechanics. 1964 Jan;18(1):1-18.

[12] Dale A Anderson, John C Tannehill, Richard H Pletcher. 9. In: Brenda M Brienza, editor. Computational Fluid Mechanics and Heat Transfer. Series in Computational Methods in Mechanics and Thermal Sciences. Hemispher Publishing Corporation; 1984. p. 507-8.

[13] Tokunaga H. Numerical simulation using vorticity-vector potential formulation. NASA Annual Research Briefs. 1993 Jan.